National University of Science and Technology
POLITEHNICA Bucharest
Doctoral School of Chemical Engineering and Biotechnologies
Field: Chemical Engineering

SUMMARY
VALORIZATION OF AGRO-INDUSTRIAL RESIDUES THROUGH PYROLYSIS

Thesis Author: Ing. Suzana Ioana STĂNCESCU (CALCAN)
PhD Supervisor: Prof. dr. ing. Oana Cristina PÂRVULESCU

2025

CONTENT

PURPOSE, CONTEXT, AND STRUCTURE OF THE THESIS 4

1. LITERATURE REVIEW 7

1.1. INTRODUCTION 7

1.2. RESIDUAL LIGNOCELLULOSIC BIOMASS 7

1.3. PRODUCTION OF BIOCHAR 8

1.3.1. TYPES OF PYROLYSIS 8

1.3.2. MECHANISMS OF LIGNOCELLULOSIC BIOMASS DECOMPOSITION DURING PYROLYSIS 8

1.3.2.1. Cellulose decomposition mechanisms 8

1.3.2.2. Hemicellulose decomposition mechanisms 8

1.3.2.3. Lignin decomposition mechanisms 8

1.3.3. FACTORS INFLUENCING THE PYROLYSIS PROCESS 8

1.3.3.1. Type and Pretreatment of the Feedstock 8

1.3.3.2. Type and Flow Rate of the Carrier Gas 9

1.3.3.3. Operating Temperature 9

1.3.3.4. Heating Rate 9

1.3.3.5. Type of Reactor 9

1.4. PHYSICOCHEMICAL PROPERTIES OF BIOCHAR 9

1.5. APPLICATIONS OF BIOCHAR 11

1.5.1. SOIL AMENDMENT 11

1.5.2. ADSORBENT FOR ENVIRONMENTAL CONTAMINANTS 11

2. ORIGINAL CONTRIBUTIONS 13

2.1. SLOW PYROLYSIS OF AGRO-INDUSTRIAL RESIDUES IN A LABORATORY-SCALE INSTALLATION 13

2.1.1. PRODUCTION AND PHYSICO-CHEMICAL CHARACTERIZATION OF BIOCHAR 13

2.1.1.1. Biochar production 13

2.1.1.2. Characterization of plant residues and biochar 17

2.1.1.3. Conclusions 23

2.1.2. PRODUCTION, CHARACTERIZATION, AND TESTING OF MODIFIED (ACTIVATED) BIOCHAR AS AN ADSORBENT BY IMPREGNATING THE RAW MATERIAL WITH ALKALINE OR ACIDIC SOLUTIONS 24

2.1.2.2. Production and testing of biochar and activated biochar as adsorbents by impregnating the raw material with phosphoric acid (H_3PO_4) solutions 24

2.1.2.3. Conclusions 29

2.2. SLOW PYROLYSIS OF AGRO-INDUSTRIAL RESIDUES IN A LABORATORY-SCALE PILOT INSTALLATION 29

2.2.1.PRODUCTION OF BIOCHAR 29

2.2.1.1. Materials, equipment, and methods 29
2.2.2. CHARACTERIZATION AND APPLICATION OF BIOCHAR AS A SOIL AMENDMENT 30
2.2.2.1. Materials, equipment, and methods 30
2.2.2.2. Results and discussion 31
2.2.3. CONCLUSIONS 36
3. GENERAL CONCLUSIONS AND RESEARCH PERSPECTIVES 37
PAPER LIST 42
SELECTIVE REFERENCES 44

PURPOSE, CONTEXT, AND STRUCTURE OF THE THESIS

Following the title, the doctoral thesis had the general objective of valorizing agro-industrial residues through slow pyrolysis, in the presence of carbon dioxide (CO_2) as a carrier agent and reactant in the process. ***The specific objectives*** of the conducted studies were to obtain, characterize, and utilize pyrolytic charcoal (biochar) produced by slow pyrolysis of residual plant materials—namely grapevine canes, grape marc, and chrysanthemum residues—as an adsorbent for air contaminants and as a soil amendment.

Vine prunings and grape marc, biodegradable residues generated in large quantities in Romania, contain relatively high concentrations of essential macro- and micronutrients for plants (Egri et al., 2022; Ion et al., 2021). Additionally, grapevine canes are currently underutilized, generally being burned (Calcan et al., 2022b). Producing biochar from biodegradable residual materials can be an effective strategy to reduce biomass waste, remediate the environment, and improve soil fertility, plant growth, development, and health.

The results presented in this thesis were obtained within the research project **372 PED BIOCHAR** (BIOCHAR FROM VEGETABLE WASTE MODIFIED FOR THE BENEFIT OF AGRONOMY AND THE ENVIRONMENT) (2020–2022); **coordinator:** National University of Science and Technology POLITEHNICA Bucharest (*project director*: Oana Cristina PÂRVULESCU); **partner:** University of Agronomic Sciences and Veterinary Medicine of Bucharest (USAMV) (***project manager***: Violeta Alexandra ION). A significant portion of the presented data has been previously published (Calcan et al., 2022a, 2022b, 2025; Egri et al., 2022; Ion et al., 2021).

The thesis comprises two main parts: **1. LITERATURE REVIEW** and 2. **ORIGINAL CONTRIBUTIONS**, complemented by general conclusions and research perspectives, a list of works, and bibliography (189 bibliographic references).

The LITERATURE REVIEW contains relevant aspects regarding the pyrolysis process, e.g., types of pyrolysis, factors influencing process performance, distribution, characterization, and applications of the products resulting from the process (biochar, bio-oil, and pyrolytic gases).

The **ORIGINAL CONTRIBUTIONS** section, which presents the results obtained from the author's research, is structured into two chapters. The first concerns the production, characterization, and testing of biochar obtained in a laboratory-scale installation. In contrast, the second focuses on the production, characterization, and testing of biochar obtained in a laboratory pilot-scale installation.

Chapter 2.1. SLOW PYROLYSIS OF AGRO-INDUSTRIAL RESIDUES IN A LABORATORY INSTALLATION contains results obtained from the slow pyrolysis of vine prunings, grape marc, and chrysanthemum residues in a pyrolysis column (3 cm inner diameter, 50 cm height) with a fixed bed of plant material, for 1 h, at 1 atm, in the presence of CO_2. This chapter is divided into two subchapters.

In **Subchapter 2.1.1. Production and physicochemical characterization of biochar**. Data are presented on the production of biochar from plant residues and the characterization of both the residues and the resulting biochar. An experimental study was conducted, based on a 2^3 factorial design, of the pyrolysis of shredded grapevine canes (average diameter × average length: 3.5 mm × 20 mm and 7.0 mm × 20 mm). The effects of process factors—namely, heat flux (q = 4244–5777 W/m²), superficial velocity of CO_2 (w = 0.4–0.8 cm/s), and volumetric mean particle diameter of plant material (d = 7–11 mm)—and their interactions were evaluated in terms of process performance indicators, i.e., final values (at τ_f = 1 h) of the specific masses of biochar and bio-oil (m_f/m_0 = 0.286−0.328 and m_{Lf}/m_0 = 0.260−0.350), as well as the average temperature of the fixed bed (t_{mf} = 401.1–486.5 °C). The plant material and biochar samples were characterized using specific analytical methods.

Subchapter 2.1.2. Production, characterization, and testing as adsorbent of modified (activated) biochar—produced by impregnating the raw material with alkaline or acidic solutions—contains data regarding the production of activated biochar via slow pyrolysis of grapevine canes impregnated with KOH or H_3PO_4 solutions, as well as its characterization and testing as an adsorbent for volatile organic compounds (VOCs) from an air stream.

Shredded vine prunings residues (average diameter × average length: 3.5 mm × 20 mm) were impregnated with KOH solutions (10%, 20%, and 30%) and H_3PO_4 solutions (10%, 31%, 48%, and 52%). Both non-impregnated and impregnated materials were pyrolyzed in the presence of CO_2 (w = 0.4 cm/s) at 1 atm.

The biochar obtained at the end of the pyrolysis process (τ_f = 1 h, q = 6.6 kW/m²) from non-impregnated residues (BC) and those impregnated with KOH solutions (10BC, 20BC, and 30BC) was characterized using specific techniques. The concentrations of carbon, hydrogen, nitrogen, oxygen, potassium, and phosphorus in BC, 10BC, 20BC, and 30BC samples were processed using Principal Component Analysis (PCA).

The biochar obtained at the end of the pyrolysis process (τ_f = 60 min, q = 4.3–6.6 kW/m², $IR = m_{acid}/m_{rez}$ = 0–2.2 g/g, where m_{acid} and m_{rez} are the masses of H_3PO_4 and plant residue, respectively) from non-impregnated (BC) and H_3PO_4-impregnated residues (ABC) was tested as an adsorbent for 1,2-dichloroethane (DCE) from an air stream. According to a CENTRAL COMPOSITE DESIGN (CCD) experimental plan with two factors (q and IR), 12 slow pyrolysis experiments were conducted. The final values (at τ_f = 60 min) of the specific masses of the solid phase (m_f/m_0 = 0.310–0.542 g/g) and liquid phase (m_{Lf}/m_0 = 0.230–0.334 g/g), as well as the average temperature of the bed of plant material (t_{mf} = 345–422 °C), were selected as responses of the pyrolysis process. The BC and ABC samples obtained in the 12 pyrolysis experiments were tested as adsorbents for VOCs (DCE) from an air stream. The final value (at $\tau_{f,ads}$ = 90 min) of the adsorption capacity of BC/ABC for the target i VOC species ($C_{if,ads}$ = 0.064–0.136 g/g) was selected as the adsorption process response. The effects of the factors and their interactions on the pyrolysis and adsorption process responses were quantified using second-order polynomial models.

Chapter 2.2. SLOW PYROLYSIS OF AGRO-INDUSTRIAL RESIDUES IN A LABORATORY PILOT-SCALE INSTALLATION contains data regarding the production of biochar in a laboratory pilot-scale installation, its characterization, and its testing as an organic soil amendment.

Strongly alkaline biochar (BC) (pH = 9.89 ± 0.01) was obtained by slow pyrolysis of shredded grapevine canes (average diameter × average length: 0.7 cm × 6 cm), using CO_2 as a carrier gas and oxidizing agent (w = 1.5 cm/s). The pyrolysis process was carried out in a furnace (inner diameter: 15.5 cm, height: 27 cm) at an average fixed-bed temperature of 517 ± 16 °C, at 1 atm, for 1 h.

The BC was ground to a diameter ≤ 2 mm and then mixed with three types of clay soils (previously ground to a diameter ≤ 2 mm), i.e., slightly alkaline alluvial soil S1 (pH = 7.99 ± 0.01), slightly acidic chernozem S2 (pH = 6.26 ± 0.02), and strongly acidic luvisol S3 (pH = 5.40 ± 0.02). The soil (S)/BC mixing ratio was 4/1 v/v, corresponding to a BC application rate of 56 t/ha. The effects of applying strongly alkaline BC on the physicochemical properties of the soils and the growth characteristics of tomato plants were evaluated.

Relevant characteristics of BC, unamended soils, and BC-amended soils—i.e., moisture content, bulk density, electrical conductivity, pH, total carbon content, concentrations of phosphorus, potassium, nitrate nitrogen, and ammonium nitrogen in soluble form, as well as concentrations of phosphorus, potassium, calcium, magnesium, and sodium in mobile form—were determined using specific methods. The results obtained from the characterization of BC,

unamended soils (S1, S2, and S3), and BC-amended soils (S1 + BC, S2 + BC, and S3 + BC) were processed using PCA.

A 66-day greenhouse experiment was conducted to assess the effects of BC on tomato (variety: oxheart) growth characteristics, i.e., plant height, number of leaves, collar diameter, and root volume. Five treatments were applied for each type of soil (15 treatments × 10 replicates per treatment): BC, foliar fertilizer (0.2 mL/100 mL water), BC + foliar fertilizer (0.2 mL/100 mL water), BC + foliar fertilizer (0.1 mL/100 mL water), and control. One-way analysis of variance (ANOVA) was used to evaluate whether the type of treatment had a significant effect ($p < 0.05$) on plant growth characteristics.

Chapter 3 presents the general conclusions of the thesis and several research perspectives.

1. LITERATURE REVIEW

1.1. INTRODUCTION

Renewable resources are an increasingly studied alternative source of energy, with residual biomass—e.g., agro-industrial, forestry, and household residues—accounting for approximately 50% of total solid waste (Chen et al., 2019; El Hanandeh et al., 2021; Ghosh et al., 2020; Kimura et al., 2010; Lee et al., 2019; Tian et al., 2023).

Numerous studies address thermochemical processes (e.g., pyrolysis, combustion, gasification) and biochemical processes (e.g., alcoholic fermentation, anaerobic fermentation) for the valorization of agro-industrial residues (Ansari et al., 2021; Biswas et al., 2017; Bridgwater, 2011; Cusenza et al., 2021; Ghosh et al., 2020; Hameed et al., 2019; Kan et al., 2016; Kimura et al., 2010; Li et al., 2020; Mlonka-Medrala et al., 2021; Tang et al., 2021; Tian et al., 2021; Usino et al., 2021; Wang et al., 2021; Yogalakshmi et al., 2022). Pyrolysis consists of the thermal decomposition of organic raw material at high temperatures (300–1300 ºC), in the absence or with a reduced supply of oxygen, resulting in biochar and a gaseous phase (i.e., a mixture of non-condensable gases, tar vapors, and water vapor), from which, after condensation, non-condensable gases and a pyrolytic liquid (bio-oil) containing 15–35% water are obtained (Bahng et al., 2009; Balat et al., 2009; Collard et al., 2014; El Bari et al., 2024; Pârvulescu et al., 2016; Yin et al., 2013).

Biochar, bio-oil, and pyrolytic gases are produced through primary devolatilization reactions of the feedstock (R1) and secondary cracking reactions of tar vapors (R2) and reforming (gasification) reactions of tar and carbon with steam (R3–R5), H_2 (R6 and R7), and CO_2 (R8 and R9) (Bru et al., 2007; Di Blasi, 1998, 2008; Garcia et al., 2000; Kechagiopoulos et al., 2006, 2007; Parihar et al., 2007; Richardson et al., 2010; Wu et al., 2007; Wu et al., 2006; Yung et al., 2009; Zanzi, 2001):

Raw material → biochar + permanent gases + vapors (tar + H_2O) (R1)

$$C_nH_m \rightarrow \frac{m}{4}CH_4 + \left(n - \frac{m}{4}\right)C \quad \text{(R2)}$$

$$C_nH_m + nH_2O \rightarrow nCO + \left(n + \frac{m}{2}\right)H_2 \quad \text{(R3)}$$

$$C_xH_yO_z + (2x - z)H_2O \rightarrow xCO_2 + \left(2x + \frac{y}{2} - z\right)H_2 \quad \text{(R4)}$$

$$C + H_2O \rightarrow CO + H_2 \quad \text{(R5)}$$

$$C_nH_m + \left(2n - \frac{m}{2}\right)H_2 \rightarrow nCH_4 \quad \text{(R6)}$$

$$C + 2H_2 \rightarrow CH_4 \quad \text{(R7)}$$

$$C_nH_m + nCO_2 \rightarrow 2nCO + \frac{m}{2}H_2 \quad \text{(R8)}$$

$$C + CO_2 \rightarrow 2CO \quad \text{(R9)}$$

1.2. RESIDUAL LIGNOCELLULOSIC BIOMASS

Residual lignocellulosic biomass is composed mainly of cellulose, hemicelluloses, and lignin, but it also contains other components (5–15%), e.g., proteins, lipids, other carbohydrates, inorganic compounds, and water (Ansari et al., 2021; Biswas et al., 2017;

Cusenza et al., 2021; Ghosh et al., 2020; Kimura et al., 2010; Li et al., 2020; Mlonka-Medrala et al., 2021; Rangabhashiyam et al., 2019; Tang et al., 2021; Tian et al., 2021; Usino et al., 2021; Wang et al., 2021).

1.3. PRODUCTION OF BIOCHAR

1.3.1. TYPES OF PYROLYSIS

Depending on the operating conditions, particularly the heating rate (v) and operating temperature (t), pyrolysis can be classified as slow (v = 0.1–1 °C/s and t = 300–700 °C), fast (v = 10–200 °C/s and t = 850–1250 °C), or flash (v > 1000 °C/s and t = 1050–1300 °C) (Bahng et al., 2009; Balat et al., 2009; Collard et al., 2014; Kim et al., 2020; Gądek et al., 2016; González et al., 2003).

1.3.2. MECHANISMS OF LIGNOCELLULOSIC BIOMASS DECOMPOSITION DURING PYROLYSIS

1.3.2.1. Cellulose decomposition mechanisms

Cellulose decomposition occurs in three stages (Collard et al., 2014):

- Formation of anhydrocellulose or active cellulose (150–300 °C)
- Depolymerization (300–390 °C)
- Rearrangement of the solid-phase structure (380–800 °C).

1.3.2.2. Hemicellulose decomposition mechanisms

1.3.2.3. Lignin decomposition mechanisms

Lignin decomposition occurs in two stages (Collard et al., 2014):

- Dehydration and fragmentation (150–420 °C)
- Fragmentation and rearrangement of the solid-phase structure (380–800 °C)

1.3.3. FACTORS INFLUENCING THE PYROLYSIS PROCESS

The distribution of products generated during pyrolysis (biochar, bio-oil, and pyrolytic gases) can be significantly affected by:

- Type and pretreatment of the feedstock
- Type and flow rate of the carrier gas
- Operating temperature
- Heating rate
- Type of pyrolysis reactor

1.3.3.1. Type and Pretreatment of the Feedstock

Biochar can be produced from a wide range of feedstocks, particularly agro-industrial and forestry residues, e.g., cereal straw, various nut shells, peanuts, rice husks, olive pits, corn cobs, fruit stones, sugarcane bagasse, sawdust, and bark of woody plants.

Before pyrolysis, feedstocks are generally pretreated through grinding and drying. They can also be chemically pretreated with different impregnating agents (Abi Bianasari et al., 2024; Kan et al., 2016; Parihar et al., 2007; Yogalakshmi et al., 2022; Yu et al., 2008; Zanzi, 2001). Chemical pretreatment of the feedstock with acid, base, and salt solutions leads to higher bio-oil yields as a result of intensified intramolecular dehydration reactions in the impregnated biomass (Çağlar and Demirbaş, 2002a, 2002b).

1.3.3.2. Type and Flow Rate of the Carrier Gas

The carrier gases used in pyrolysis can be inert, e.g., Ar, N_2, or act as reactants in the process, e.g., steam, CO_2. Steam and CO_2 are oxidizing agents frequently used as carrier gases (Zanzi, 2001).

1.3.3.3. Operating Temperature

On the one hand, at operating temperatures below 500 °C, the yields of bio-oil and pyrolytic gases increase with increasing temperature. On the other hand, at temperatures above 500 °C, the bio-oil yield decreases, while the yield of pyrolytic gases increases with increasing temperature, as a result of intensified thermal cracking reactions (R2) and reforming with H_2, CO_2, and water vapor (R3–R9) (Acikgoz et al., 2004; Çağlar and Demirbaş, 2002a, 2002b; Damartzis et al., 2008; Demirbaş, 2002a, 2002b, 2006; Di Blasi et al., 1999; Gonzalez et al., 2003; Parihar et al., 2007; Xiu et al., 2006; Zabaniotou and Ioannidou, 2008; Zanzi, 2001).

1.3.3.4. Heating Rate

In general, higher heating rates result in lower biochar yields and higher amounts of volatile compounds (permanent gases and vapors) (González et al., 2003; Xiu et al., 2006; Yogalakshmi et al., 2022; Zanzi, 2001).

1.3.3.5. Type of Reactor

Several types of pyrolysis reactors can be used, i.e.:

- Fixed bed biomass reactors (in the presence of a carrier gas or under vacuum);
- Fluidized bed biomass reactors;
- Circulating fluidized bed reactors;
- Rotary kilns;
- Rotating cone reactors (centrifugal type);
- Screw conveyor reactors.

In general, fixed bed and screw conveyor reactors are used for producing biochar via slow pyrolysis, whereas fluidized bed, rotary, and centrifugal-type reactors are used for producing bio-oil via fast/flash pyrolysis (Verma et al., 2012).

1.4. PHYSICOCHEMICAL PROPERTIES OF BIOCHAR

Relevant physicochemical properties of biochar used in various applications include: particle size, density, pore size, porosity and specific surface area, moisture content, ash content, volatile matter and elemental composition, electrical conductivity, pH, type and number of functional groups, cation exchange capacity, and water holding capacity (Chen et al., 2019; Calcan et al., 2022a).

The particle size of BC depends on the heating rate, as well as on the type and size of the raw material particles. In general, at low heating rates, the particle sizes of BC and the raw material are similar, whereas at high heating rates, volatile compounds from the raw material are rapidly removed, causing particle fragmentation.

The density of BC, which refers either to bulk density (the density of the fixed bed of particles) or particle density, varies depending on the raw material used and the operating conditions (Vandana et al., 2025). In general, BC with a high ash content and that obtained at higher temperatures have higher density values (Collard et al., 2014). Typically, bulk density values of BC range from 0.1 to 1.7 g/cm³, while particle density values range from 0.3 to 1.8 g/cm³ (Brewer & Levine, 2015; Dayoub et al., 2024).

The pore size, porosity, and Brunauer-Emmett-Teller (BET) specific surface area (SSA) of BC particles are determined using mercury porosimetry. Pore size can also be estimated using scanning electron microscopy (SEM). Depending on their size, pores are classified into

three categories, i.e., micropores (with a diameter less than 2 nm), mesopores (with a diameter between 2 and 50 nm), and macropores (with a diameter greater than 200 nm).

The porosity and SSA of BC are particularly important factors in specific applications, e.g., environmental remediation (Brewer, 2012). In general, depending on the type of raw material and operating conditions, BC has porosity values ranging from 0.30 to 0.85 and SSA values ranging from 1 to 500 m^2/g (Chen et al., 2019a; Dayoub et al., 2024; Wystalska & Kwarciak-Kozłowska, 2021). SSA increases with rising temperature; however, excessive temperature increase leads to a decrease in SSA due to the destruction of micropores (Chen et al., 2019).

Water, ash, and volatile matter concentrations are determined by gravimetric methods, while the concentrations of C, H, O, N, and S (denoted C, H, O, N, and S) are determined by elemental analysis. Mineral concentrations, e.g., N, P, K, Ca, Mg, S, Na, Al, B, Cl, Co, Cr, Cu, Fe, Mn, Mo, Ni, and Zn (denoted N, P, K, Ca, Mg, S, Na, Al, B, Cl, Co, Cr, Cu, Fe, Mn, Mo, Ni, Zn), are measured using inductively coupled plasma optical emission spectrometry (ICP-OES) and inductively coupled plasma mass spectrometry (ICP-MS) (subchapter 2.1.1.2.1).

The electrical conductivity (EC) of BC is significantly influenced by pyrolysis conditions (especially the type and pretreatment of the feedstock, temperature, heating rate, and residence time) (Vandana et al., 2025). EC increases with pyrolysis temperature due to the enhanced degree of aromaticity of the porous structure, and generally, EC values range between 10^{-2}–10^{2} S/cm (10^{-1}–10^{3} dS/m) (Kane et al., 2021).

In general, BC is alkaline, and its pH increases with temperature, due to the decomposition of carboxylic, hydroxyl, or phenolic groups and the volatilization of organic acids (Chen et al., 2019a). Its pH also significantly influences the physical and chemical properties of the soil; therefore, the correct selection of BC type for soil amendment is extremely important (Brewer, 2012).

The type and number of functional groups are key factors determining BC applications (Vandana et al., 2025). The number of functional groups depends on the operating temperature, i.e., increasing temperature raises the number of C–O and C–H bonds while decreasing the number of O–H bonds (Chen et al., 2019). The type of functional groups is influenced by both the feedstock and operating conditions. The hydrophobic and hydrophilic regions on the BC surface can retain both polar and nonpolar molecules from the environment.

The biomass type and pyrolysis temperature significantly influence the cation exchange capacity (CEC) of BC. At lower operating temperatures, certain functional groups—especially hydroxyl, carbonyl, and carboxyl—are preserved within the porous structure (due to the incomplete decomposition of cellulose), leading to an increase in CEC. A higher content of alkaline metals can also result in greater CEC values (Chen et al., 2019a).

Water holding capacity (WHC) is a significant property of BC used as a soil amendment. WHC depends on the type and pretreatment of the feedstock, particle size, and operating conditions—particularly the operating temperature, type, and flow rate of the carrier gas. Increasing operating temperature improves the degree of aromaticity and hydrophobicity of the porous structure, reduces the number of O- and H-containing functional groups, and thus decreases WHC (Chen et al., 2019a; Vandana et al., 2025; Zhang et al., 2023). Due to its high porosity and SSA values, BC can retain large amounts of water, i.e., WHC values can exceed 400% (g water/100 g BC), releasing it gradually to plants, which can have significant beneficial effects on their growth and development (Khater et al., 2024).

BC properties can be improved through physical or chemical activation (e.g., physical activation with CO_2 or steam, chemical modification with acids, bases, metal salts, or oxides), resulting in activated BC (ABC) with tailored properties for specific applications (Di Blasi et al., 2009; Gwenzi et al., 2021; Premarathna et al., 2019; Rajapaksha et al., 2016; Wang et al., 2017; Wang & Wang, 2019; Zhang et al., 2022).

1.5. APPLICATIONS OF BIOCHAR

BC is a low-cost, renewable resource that is easy to produce, and therefore has multiple applications, e.g., as a soil amendment, adsorbent for contaminants in soil, water, and air, catalyst/catalyst support, and fuel. A product with a high nutrient content and relatively high porosity and SSA values can be used as a soil amendment. BC produced at higher temperatures ($t > 500$ °C), which has high porosity, SSA, pH, and C content, a high degree of aromaticity, and low polarity (due to the pronounced removal of O- and H-containing functional groups), is effective for the removal of nonpolar organic contaminants. In contrast, BC produced at lower temperatures ($t < 500$ °C), which contains more O- and H-containing functional groups and is less porous, is recommended for the removal of polar organic contaminants and inorganic compounds (Amalina et al., 2022; Oliveira et al., 2017; Yaashikaa et al., 2020).

1.5.1. SOIL AMENDMENT

The application of biochar (biochar, BC) as a soil amendment can significantly improve soil quality by neutralizing pH, increasing cation exchange capacity (CEC), specific surface area (SSA), water holding capacity (WHC), and nutrient content, as well as by enhancing microbial and enzymatic activity in the soil. Soils amended with BC have a lower bulk density (BD), which has positive effects on plant growth due to improved root development, and therefore better water and nutrient uptake (Yaashikaa et al., 2020). BC also contributes to improving carbon sequestration in soil, retaining greenhouse gas emissions, and reducing nutrient leaching, thus enhancing soil fertility and health (Purakayastha et al., 2019; Qian et al., 2015). The positive effect of BC on plant growth and development has been demonstrated in many studies from the literature.

1.5.2. ADSORBENT FOR ENVIRONMENTAL CONTAMINANTS

Biochar (BC) and physically or chemically activated biochar (ABC) can be effective adsorbents for organic and inorganic contaminants in soil, water, and air—pollutants that, even at low concentrations, can significantly impact ecosystems (Sizmur et al., 2017). The adsorption capacity of BC/ABC for different contaminants depends on (Zhao et al., 2022):

- the characteristics of BC/ABC (especially pore size, porosity, specific surface area, mineral content, pH, and the type and number of functional groups) and the properties of the contaminant species;
- pyrolysis process factors, i.e., feedstock type and pretreatment, feedstock particle size, heating rate, type and flow rate of carrier gas, operating temperature and duration, and activation conditions;
- adsorption process factors.

BC/ABC can retain (mainly through physical or chemical adsorption) various types of organic contaminants, e.g., volatile organic compounds (VOCs), cationic dyes (methylene blue, rhodamine), emerging contaminants (food additives, flame retardants, persistent organic pollutants, pharmaceuticals and personal care products, pesticides) (Bedia et al., 2018; Yaashikaa et al., 2020).

The activation process can significantly influence the properties of ABC and, consequently, its adsorption capacity. Physical activation with oxidizing gases (CO_2 or steam) introduces O-containing functional groups and creates numerous pores in the material structure, particularly micropores (Wang et al., 2017; Zhao et al., 2022). O-containing functional groups facilitate the adsorption of inorganic contaminants and polar organic contaminants (Gwenzi et al., 2021; Oliveira et al., 2017). Chemical treatment with acids

(HNO_3, HCl, H_2SO_4, H_3PO_4), bases (KOH, NaOH), metal salts ($MgCl_2$, $ZnCl_2$, $AlCl_3$, $FeCl_3$, K_2CO_3), or oxides (CaO, MgO, MnO, ZnO, TiO_2, Fe_2O_3), carried out either before or after pyrolysis, generally promotes the formation of micropores, increases SSA and the number of surface functional groups, thereby improving the adsorption capacity of ABC (Pimentel et al., 2023; Sajjadi et al., 2018; Wang et al., 2017; Wang & Wang, 2019; Wang et al., 2021; Xu et al., 2020; Zhang et al., 2022; Zhao et al., 2022; Zhu et al., 2018).

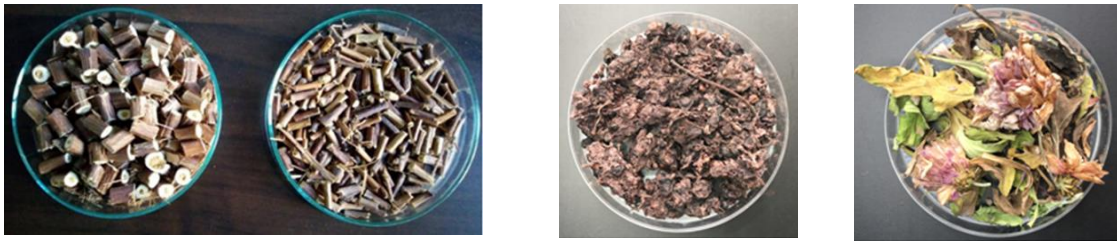
2. ORIGINAL CONTRIBUTIONS

2.1. SLOW PYROLYSIS OF AGRO-INDUSTRIAL RESIDUES IN A LABORATORY-SCALE INSTALLATION

2.1.1. PRODUCTION AND PHYSICO-CHEMICAL CHARACTERIZATION OF BIOCHAR

2.1.1.1. Biochar production

Vine prunings, grape pomace, and chrysanthemum residues (*Chrysanthemum morifolium* Ramat) were used as raw materials in the pyrolysis process. The plant materials were ground and oven-dried prior to pyrolysis (Figure 14).



a b c

Figure 14. Ground and dried plant materials: (a) coarsely and finely cut vine pruning; (b) grape pomace; (c) chrysanthemum residues (Calcan et al., 2022a; Ion et al, 2021).

Slow pyrolysis of plant residues was carried out at POLITEHNICA University of Bucharest, Department of Chemical and Biochemical Engineering, using the experimental setup shown in Figure 15.

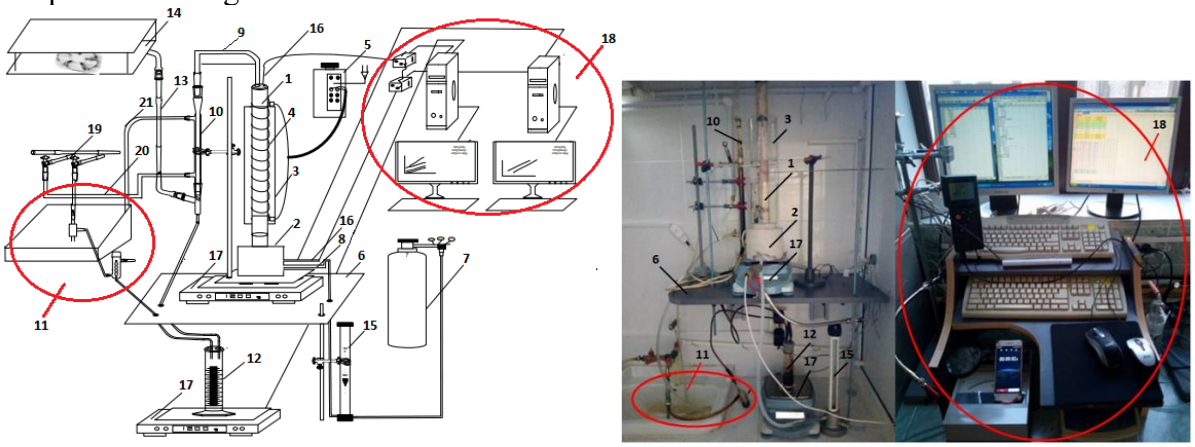


Figure 15. Experimental setup: (1) pyrolysis column; (2) autoclaved cellular concrete (ACC) support; (3) glass cylinder (jacket); (4) electric resistance; (5) autotransformer; (6) melamine board; (7) CO_2 tank; (8) CO2 feed pipe; (9) pipe collecting volatile products; (10) Liebig condenser; (11) laboratory vacuum system; (12) oil collector; (13) pipe collecting non-condensable gases; (14) exhaust hood; (15) flow-meter; (16) thermocouples; (17) electronic balances; (18) data acquisition system; (19) water source; (20) cold water (thermal agent in condenser) feed pipe; (21) water outlet pipe.

The biomass was fed into the ceramic column (1), with an inner diameter (D) of 0.03 m and a height of 0.5 m, which was fixed in a support made of autoclaved aerated concrete (AAC) (2). The column wall (4 mm thick), thermally insulated by a glass cylinder (3), was heated by an electric heater (4), powered by an autotransformer (5). The pyrolysis column was mounted on a melamine support (6) fixed to the walls of a laboratory niche. Carbon dioxide (CO_2) supplied from the cylinder (7) was introduced into the column (1) via the inlet pipe (8).

The CO_2 flowed upward through the fixed bed of biomass, carrying the volatile compounds produced during pyrolysis, which were subsequently removed through the collection pipe (9). The resulting mixture of non-condensable gases and vapors was cooled in a shell-and-tube heat exchanger (10), yielding bio-oil and non-condensable gases. Volatile compounds were evacuated and condensed under vacuum conditions utilizing a vacuum system (11). The pyrolytic liquid was collected in a graduated cylinder (12), while non-condensable gases were vented through the outlet pipeline (13) and laboratory fume hood (14).

The volumetric flow rate of CO_2, G_V (m^3/s), was monitored by a flowmeter (15). Temperatures at the center of the biomass bed (t_c) and the column wall (t_w) were recorded using thermocouples (16). The masses of solid (m) and liquid (m_L) phases were measured continuously with electronic balances (17). All temperature and mass data were acquired in real-time via a data acquisition system (18). The pyrolysis experiments were conducted at atmospheric pressure (1 atm), with a duration (τ_f) of 1 hour.

The heat flux, q (W/m^2), the superficial velocity of CO_2, w (m/s), defined by equation (1), and the average particle diameter of the plant material, d (m), were selected as the independent variables (factors) of the process. The specific masses of the solid and liquid phases, m/m_0 and m_L/m_0, where m_0 (g) represents the initial mass of the plant material, and the logarithmic mean temperature of the plant material layer, t_m (°C), defined by equation (2), were selected as the dependent variables (responses) of the process.

$$w = \frac{4G_V}{\pi D^2} \tag{1}$$

$$t_m = \frac{t_w - t_c}{\ln\left(\frac{t_w}{t_c}\right)} \tag{2}$$

According to a 2^3 factorial design, eight slow pyrolysis experiments (1–8 in Table 3) on vine prunings were conducted at two levels (minimum and maximum) of the factors.

Table 3. Factor levels and process performance in the pyrolysis of vine prunings.

Exp.	q (W/m^2)	w (m/s)	d (m)	x_1	x_2	x_3	m_f/m_0	m_{Lf}/m_0	t_{mf} (°C)
1	4244	0.004	0.007	-1	-1	-1	0.312	0.278	426.6
2	5777	0.004	0.007	1	-1	-1	0.306	0.328	473.6
3	4244	0.008	0.007	-1	1	-1	0.328	0.260	401.1
4	5777	0.008	0.007	1	1	-1	0.324	0.346	449.2
5	4244	0.004	0.011	-1	-1	1	0.298	0.296	406.9
6	5777	0.004	0.011	1	-1	1	0.286	0.350	486.5
7	4244	0.008	0.011	-1	1	1	0.314	0.328	406.3
8	5777	0.008	0.011	1	1	1	0.310	0.304	479.1
9	5010	0.006	0.009	0	0	0	0.312	0.306	438.8
10	5010	0.006	0.009	0	0	0	0.309	0.312	442.7
11	5010	0.006	0.009	0	0	0	0.305	0.314	444.2

2.1.1.1.2. Results and discussion

The time (τ) variations of the experimentally determined dependent variables (responses) (m/m_0, m_L/m_0, and t_m) are presented in Figures 16–18. The performance of the vine prunings pyrolysis process, i.e., the final values (at τ_f= 1 h) of the dependent variables, is shown in Table 3. The data presented in Figures 16–18 and Table 3 generally indicate the following aspects:

- The values of the average temperature of the material layer (t_m) and the specific mass of bio-oil (m_L/m_0) are higher, while those of the specific mass of the solid phase (m/m_0) are lower at the higher heat flux level (q = 5777 W/m²);
- The values of m_L/m_0 are higher and those of m/m₀ are lower at a larger particle size (d = 0.011 m) and a lower superficial velocity of CO_2 (w = 0.004 m/s);
- The diameter d has a negligible influence on the average temperature t_m, and the effect of the superficial velocity w on t_m is negligible for coarse particles (d = 0.011 m);
- The final values of the layer temperature (t_{mf}) are higher, and those of the specific mass of the solid phase (m_f/m_0) are lower at the higher levels of parameters q and d, as well as at the lower level of the superficial velocity w;
- The final values of the specific mass of bio-oil (m_{Lf}/m_0) are higher at the higher levels of parameters q and d

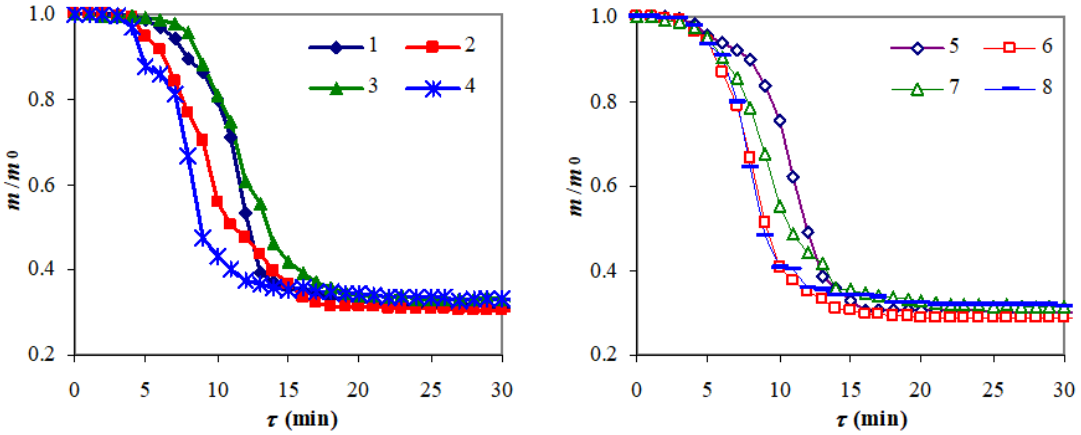


Figure 16. Specific mass of solid as a function of time (Calcan et al., 2022a).

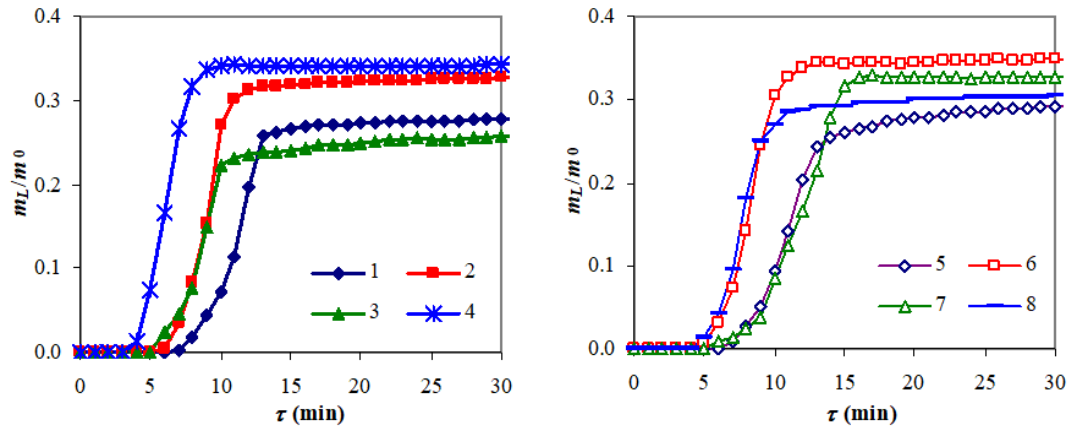


Figura 17. Specific mass of bio-oil as a function of time (Calcan et al., 2022a).

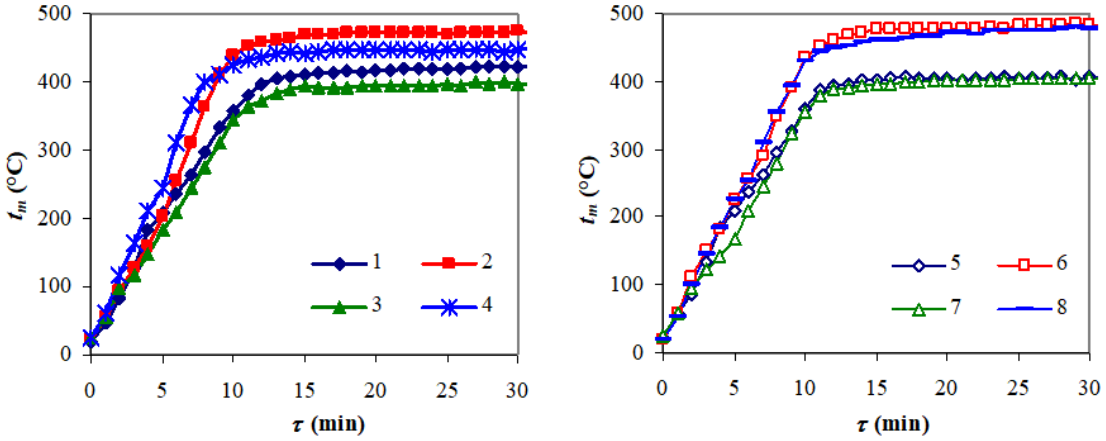


Figura 18. Average temperature of the fixed bed of plant material as a function of time (Calcan et al., 2022a).

Processing of experimental data

The performance of vine prunings pyrolysis was estimated as a function of the dimensionless process factors using multiple regression equations. The dimensionless factors (x_j, j = 1..3) are defined by equations (4)–(6). To test the significance of the regression coefficients, three experiments at the center of the experimental design (experiments 9–12 in Table 3) were conducted. The effects of the factors x_j (j = 1..3) and their interactions (x_1x_2, x_1x_3, x_2x_3 și $x_1x_2x_3$) on the responses y_i (i = 1..3) were quantified using statistical models described by equations (7)–(9), where $y_1 = (m_f/m_0)_{calc}$, $y_2 = (m_{Lf}/m_0)_{calc}$ and $y_3 = t_{mf,calc}$ are the process performances, and β_{ki} (k = 1..8, i = 1..3) are the regression coefficients. The regression coefficients β_{ki},, determined based on the experimental data from Table 3, are presented in Tables 4–6 along with the values of the standard errors (SE_{ki}), Student's t-statistics (t_{ki}), p-values (p_{ki}), coefficient of determination (R^2), adjusted R^2 (R^2_{adj}), regression standard error (RSE), Fisher's F-statistic (F), and its corresponding p-value (for F). Statistically significant coefficients (pki ≤ α = 0.05, where α is the significance level) in Tables 4–6 are highlighted in bold. The tabulated results indicate that the experimental data and those calculated using equations (7)–(9) are in good agreement ($R^2 \geq 0{,}979$, $R^2_{adj} \geq 0{,}930$, $RSE \leq 23{,}62$, $F \geq 20{,}08$ and $p \leq 0{,}016$).

$$x_1 = \frac{q - 5010}{766} \tag{4}$$

$$x_2 = \frac{w - 0{,}006}{0{,}002} \tag{5}$$

$$x_3 = \frac{d - 0{,}009}{0{,}002} \tag{6}$$

$$y_1 = 0{,}3095 + 0{,}0093x_2 - 0{,}0078x_3 + 0{,}0013x_1x_2 - 0{,}0008x_1x_3 + 0{,}0008x_2x_3 + 0{,}0008x_1x_2x_3 \tag{7}$$

$$y_2 = 0{,}3111 - 0{,}0018x_2 + 0{,}0082x_3 - 0{,}0052x_1x_2 - 0{,}0133x_1x_3 - 0{,}0018x_2x_3 - 0{,}0143x_1x_2x_3 \tag{8}$$

$$y_3 = 441{,}4 - 7{,}2218x_2 + 3{,}5258x_3 - 0{,}7164x_1x_2 + 7{,}1628x_1x_3 + 5{,}2413x_2x_3 - 0{,}9845x_1x_2x_3 \tag{9}$$

$$y_1 = 0{,}3095 + 0{,}0093x_2 - 0{,}0078x_3 \tag{10}$$

Table 4. Results of the multiple regression analysis for y_1 defined by equation (7)

	k	β_{k1}	SE_{k1}	t_{k1}	p_{k1}
Intercept	1	**0.3095**	0.0009	340.68	6.0E-08
x_1	2	0.0000	0.0011	0.0000	1.0000
x_2	3	**0.0093**	0.0011	8.6845	0.0032
x_3	4	**-0.0078**	0.0011	-7.2762	0.0054
x_1x_2	5	0.0013	0.0011	1.1736	0.3253
x_1x_3	6	-0.0008	0.0011	-0.7041	0.5321
x_2x_3	7	0.0008	0.0011	0.7041	0.5321
$x_1x_2x_3$	8	0.0008	0.0011	0.7041	0.5321
R^2	0.979				
R^2_{adj}	0.930				
RSE	0.003				
F	20.08				
p	0.016				

Table 5. Results of the multiple regression analysis for y_2 defined by equation (8).

	k	β_{k2}	SE_{k2}	t_{k2}	p_{k2}
Intercept	1	**0.3111**	0.0010	300.32	8.0E-08
x_1	2	0.0000	0.0012	0.0000	1.0000
x_2	3	-0.0018	0.0012	-1.4407	0.2453
x_3	4	**0.0082**	0.0012	6.7921	0.0065
x_1x_2	5	**-0.0052**	0.0012	-4.3222	0.0228
x_1x_3	6	**-0.0133**	0.0012	-10.909	0.0016
x_2x_3	7	-0.0018	0.0012	-1.4407	0.2453
$x_1x_2x_3$	8	**-0.0143**	0.0012	-11.732	0.0013
R^2	0.995				
R^2_{adj}	0.984				
RSE	0.003				
F	88.20				
p	0.002				

Table 6. Results of the multiple regression analysis for y3 defined by equation (9).

	k	β_{k3}	SE_{k3}	t_{k3}	p_{k3}
Termen liber	1	**441.36**	0.7123	619.67	9.0E-09
x_1	2	0.0000	0.8352	0.0000	1.0000
x_2	3	**-7.2218**	0.8352	-8.6469	0.0033
x_3	4	**3.5258**	0.8352	4.2215	0.0243
x_1x_2	5	-0.7164	0.8352	-0.8578	0.4541
x_1x_3	6	**7.1628**	0.8352	8.5763	0.0033
x_2x_3	7	**5.2413**	0.8352	6.2756	0.0082
$x_1x_2x_3$	8	-0.9845	0.8352	-1.1788	0.3234
R^2	0.998				
R^2_{adj}	0.994				
RSE	2.362				
F	225.5				
p	4.5E-04				

2.1.1.2. Characterization of plant residues and biochar

The plant residue and biochar samples were analyzed at the Research Center for the Study of Agri-Food Product Quality (USAMV). All analyses were performed in triplicate. The following parameters were determined: dry matter content, *DM* (%); ash content, *Ash* (%); volatile matter content, *VM* (%); fixed carbon content, *FC* (%); percentage concentrations of carbon (*C*), hydrogen (*H*), nitrogen (*N*), sulfur (*S*), and oxygen (*O*); bulk density, *BD* (g/cm³); electrical conductivity (*EC*); *pH*; water holding capacity (*WHC*) (Table 11); morphology and functional groups (Figures 24-26, Table 14); and the content of *Ca, K, P, Mg, Fe, Al, Mn, Zn, B, Cu, Co,* and *Mo* (Table 12 and 13).

2.1.1.2.2. Results and discussion

The tabulated data indicate the following aspects: (i) The biochar derived from grape pomace (BC-T) exhibits higher levels of dry matter content (*DM*), fixed carbon (*FC*), nitrogen concentration (*N*), bulk density (*BD*), and *pH*, but lower levels of volatile matter content (*VM*) and oxygen concentration (*O*) compared to the biochar obtained from chrysanthemum residues (BC-C);(ii) The biochar produced from vine prunings (BC-V) shows higher carbon concentration (*C*), but lower electrical conductivity (*EC*), ash content (*Ash*), and hydrogen concentration (*H*) than that derived from grape pomace (BC-T). The low *BD* values (0.10–0.28 g/cm³), along with the relatively high *pH* values (10.16–11.24) and water holding capacity (*WHC*) (43.25–72.02%), support the use of biochar as a soil amendment for acidic soils.

Table 11. Physico-chemical properties of biochar obtained from ground vine prunings (BC-V), grape pomace (BC-T), and chrysanthemum residues (BC-C).

	DM (%)	*VM* (%)	*Ash* (%)	*FC* (%)	*C* (%)	*H* (%)	*N* (%)	*O* (%)	*BD* (g/cm^3)	*EC* (dS/m)	*pH*	*WHC* (%)
BC-V	98.21	31.84	7.29	59.09	70.69	3.59	2.36	23.36	0.11	0.52	10.39	61.60
	98.62	34.07	7.94	56.62	70.26	3.64	2.30	23.80	0.11	0.55	10.37	43.36
	97.60	30.95	8.47	58.18	70.66	3.53	2.35	23.46	0.11	0.58	10.28	72.02
m	**98.14**	**32.29**	**7.90**	**57.96**	**70.54**	**3.59**	**2.34**	**23.54**	**0.11**	**0.55**	**10.35**	**58.99**
s	**0.51**	**1.61**	**0.59**	**1.25**	**0.24**	**0.05**	**0.03**	**0.23**	**0.00**	**0.03**	**0.06**	**14.51**
***CV* (%)**	**0.52**	**4.98**	**7.48**	**2.16**	**0.34**	**1.51**	**1.41**	**0.99**	**1.27**	**5.61**	**0.57**	**24.59**
BC-T	99.21	37.19	16.40	45.63	70.04	4.39	2.39	23.18	0.22	4.09	11.24	60.75
	99.30	36.70	18.30	44.30	69.00	3.95	2.81	24.24	0.25	3.85	11.22	45.60
	99.23	34.22	16.31	48.69	68.16	4.40	2.56	24.88	0.28	3.68	11.20	62.13
m	**99.25**	**36.04**	**17.00**	**46.21**	**69.07**	**4.25**	**2.58**	**24.10**	**0.25**	**3.88**	**11.22**	**56.16**
s	**0.05**	**1.59**	**1.12**	**2.25**	**0.94**	**0.26**	**0.21**	**0.86**	**0.03**	**0.21**	**0.02**	**9.17**
***CV* (%)**	**0.05**	**4.42**	**6.61**	**4.87**	**1.37**	**6.05**	**8.16**	**3.58**	**11.99**	**5.34**	**0.21**	**16.33**
BC-C	96.28	46.92	27.24	22.11	69.69	3.72	1.30	25.29	0.10	1.39	10.16	43.25
	96.31	44.75	19.63	31.93	68.66	3.70	1.43	26.22	0.11	1.32	10.27	68.06
	96.42	44.53	17.18	34.71	68.93	3.78	1.59	25.70	0.10	1.36	10.17	67.27
m	**96.34**	**45.40**	**21.35**	**29.58**	**69.09**	**3.73**	**1.44**	**25.74**	**0.11**	**1.35**	**10.20**	**59.53**
s	**0.07**	**1.32**	**5.25**	**6.62**	**0.54**	**0.04**	**0.15**	**0.47**	**0.01**	**0.03**	**0.06**	**14.10**
***CV* (%)**	**0.08**	**2.91**	**24.57**	**22.38**	**0.78**	**1.15**	**10.22**	**1.81**	**5.22**	**2.50**	**0.59**	**23.69**

Table 12. ICP-OES analysis results for biochar obtained from ground vine prunings (BC-V), grape pomace (BC-T), and chrysanthemum residues (BC-C).

	Ca	*P*	*K*	*Zn*	*Al*	*B*	*Cu*	*Fe*	*Mg*	*Mn*
	(mg/kg)									
BC-V	14658.97	6238.22	44003.27	79.47	17.33	17.08	13.78	44.71	2660.17	22.50
	14456.91	6052.85	41945.20	79.67	17.41	16.54	13.89	44.93	2610.02	22.66
	14450.16	6135.38	41124.56	78.46	17.10	15.58	13.73	44.40	2625.76	22.37
***m* (mg/kg)**	**14522.01**	**6142.15**	**42357.68**	**79.20**	**17.28**	**16.40**	**13.80**	**44.68**	**2631.98**	**22.51**
***s* (mg/kg)**	**118.66**	**92.87**	**1483.02**	**0.65**	**0.16**	**0.76**	**0.08**	**0.27**	**25.65**	**0.15**
***CV* (%)**	**0.82**	**1.51**	**3.50**	**0.82**	**0.93**	**4.63**	**0.59**	**0.60**	**0.97**	**0.65**
BC-T	13081.30	7872.50	60414.10	30.00	282.30	86.20	38.70	452.10	1930.40	52.10
	13368.90	7805.50	60381.80	30.20	282.70	88.10	39.10	452.60	1954.50	52.10
	13303.10	7826.50	61512.40	30.00	280.20	87.50	38.80	448.90	1912.60	51.60
***m* (mg/kg)**	**13251.10**	**7834.83**	**60769.43**	**30.07**	**281.73**	**87.27**	**38.87**	**451.20**	**1932.50**	**51.93**
***s* (mg/kg)**	**150.69**	**34.27**	**643.63**	**0.12**	**1.34**	**0.97**	**0.21**	**2.01**	**21.03**	**0.29**
***CV* (%)**	**1.14**	**0.44**	**1.06**	**0.38**	**0.48**	**1.11**	**0.54**	**0.44**	**1.09**	**0.56**
BC-C	9252.93	4058.75	74127.16	42.60	205.04	20.63	14.71	169.33	1135.59	29.81
	9254.10	4021.69	69908.04	42.85	204.67	19.33	14.82	170.87	1111.29	30.05
	9079.90	3965.06	65457.71	42.71	200.83	18.39	14.74	169.90	1106.29	29.89
***m* (mg/kg)**	**9195.64**	**4015.17**	**69830.97**	**42.72**	**203.51**	**19.45**	**14.76**	**170.03**	**1117.72**	**29.92**
***s* (mg/kg)**	**100.24**	**47.19**	**4335.24**	**0.13**	**2.33**	**1.12**	**0.06**	**0.78**	**15.67**	**0.12**
***CV* (%)**	**1.09**	**1.18**	**6.21**	**0.30**	**1.14**	**5.78**	**0.37**	**0.46**	**1.40**	**0.41**

Table 13. ICP-MS analysis results for biochar obtained from ground vine prunings (BC-V), grape pomace (BC-T), and chrysanthemum residues (BC-C).

	Co (mg/kg)	*Mo* (mg/kg)		*Co* (mg/kg)	*Mo* (mg/kg)		*Co* (mg/kg)	*Mo* (mg/kg)
BC-V	0.017	2.295	BC-T	0.089	0.356	BC-C	0.094	0.451
	0.017	2.332		0.091	0.365		0.094	0.45
	0.017	2.307		0.088	0.354		0.092	0.443
***m* (mg/kg)**	**0.017**	**2.311**	***m***	**0.089**	**0.358**	***m***	**0.093**	**0.448**
***s* (mg/kg)**	**0.000**	**0.019**	***s* (mg/kg)**	**0.002**	**0.006**	***s* (mg/kg)**	**0.001**	**0.004**
***CV* (%)**	**0.000**	**0.817**	***CV* (%)**	**1.710**	**1.635**	***CV* (%)**	**1.237**	**0.973**

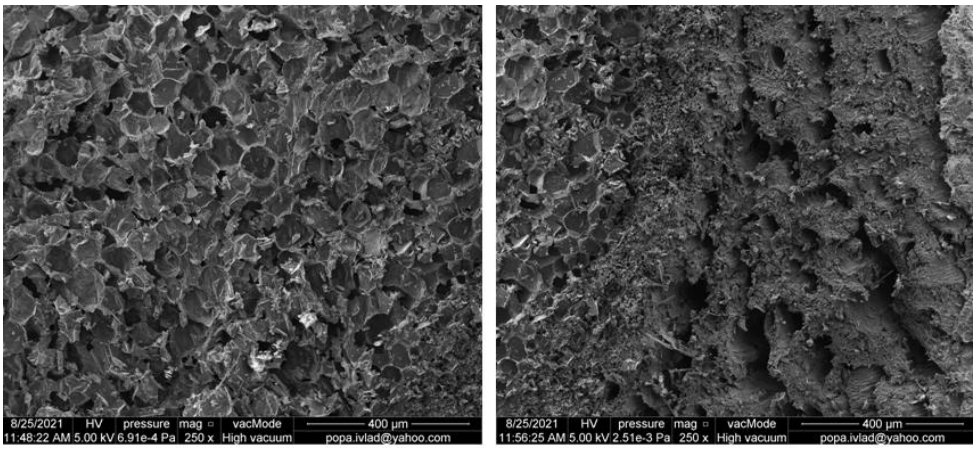


Figure 24. SEM images of biochar obtained from vine prunings (BC-V).

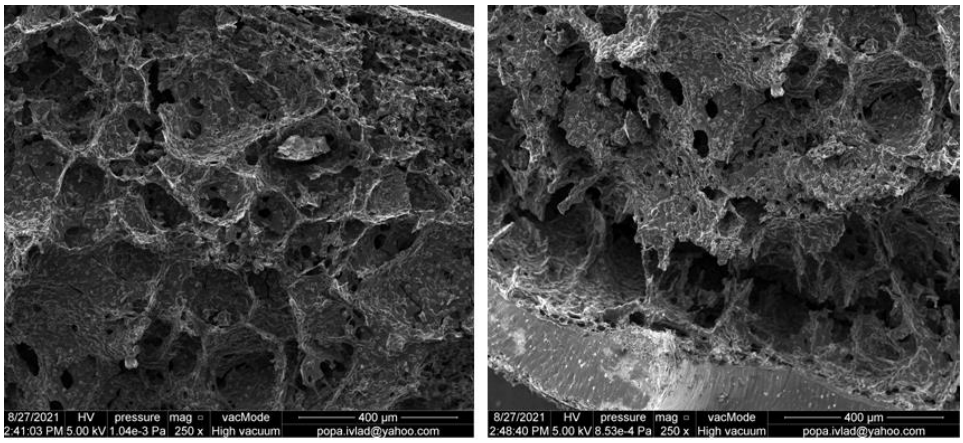


Figure 25. SEM images of biochar obtained from grape pomace (BC-T).

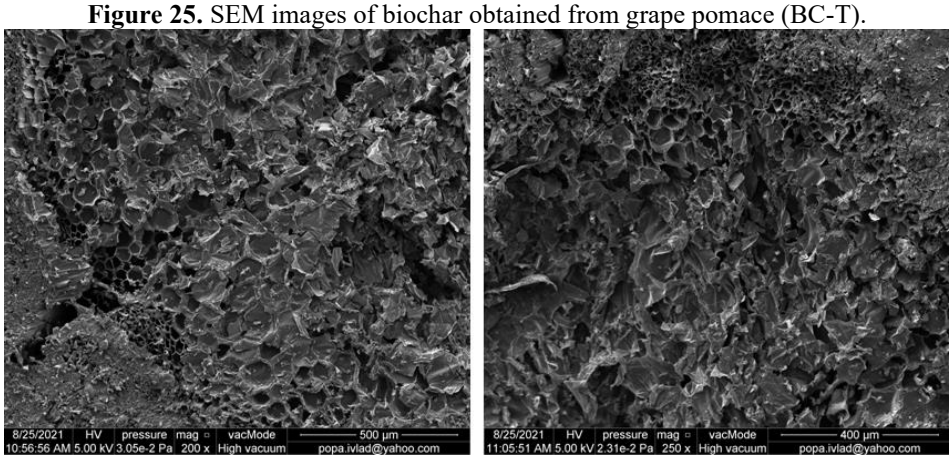


Figure 26. SEM images of biochar obtained from chrysanthemum residues (BC-C).

Table 14. Functional groups and corresponding vibrations of relevant peaks from the FT-IR spectra of biochar obtained from vine prunings (BC-V), grape pomace (BC-T), and chrysanthemum residues (BC-C)

No.	BC-V	BC-T	BC-C	Functional group/vibration
1	3198.89	-	3200.08	O−H / stretching
2	-	2921.52	-	C−H (methyl or methylene from aliphatic compounds) / stretching
3	1578.95	1563.75	1561.06	C=C (from aromatic ring) / stretching
4	-	-	1370.64	C−H (methyl from aliphatic compounds) / bending
5	1314.45	1315.84	-	C−O (attached to aromatic ring) / stretching
6	755.87	-	1023.18	C−H (attached to aromatic ring) / bending

Processing of experimental data

The results of the physicochemical analyses for the raw materials and the obtained biochar were processed using principal component analysis (PCA).

Table 22. Coordinates of variables on factors PC1, PC2, and PC3 for biochar samples obtained from vine prunings (BC-V), grape pomace (BC-T), and chrysanthemum residues (BC-C).

No.	Variable symbol	PC1	PC2	PC3
1	*DM*	**0.979**	-0.092	-0.136
2	*VM*	**-0.812**	-0.536	-0.121
3	*Ash*	-0.497	**-0.797**	-0.237
4	*FC*	**0.730**	0.646	0.163
5	*C*	0.139	**0.831**	-0.341
6	*H*	0.552	**-0.739**	0.132
7	*N*	**0.966**	0.101	-0.012
8	*O*	**-0.747**	-0.517	0.248
9	*BD*	**0.747**	-0.647	0.064
10	*EC*	0.564	**-0.800**	-0.005
11	*pH*	**0.821**	-0.557	-0.016
12	*WHC*	-0.067	0.179	**0.938**

Significant values are highlighted in bold.

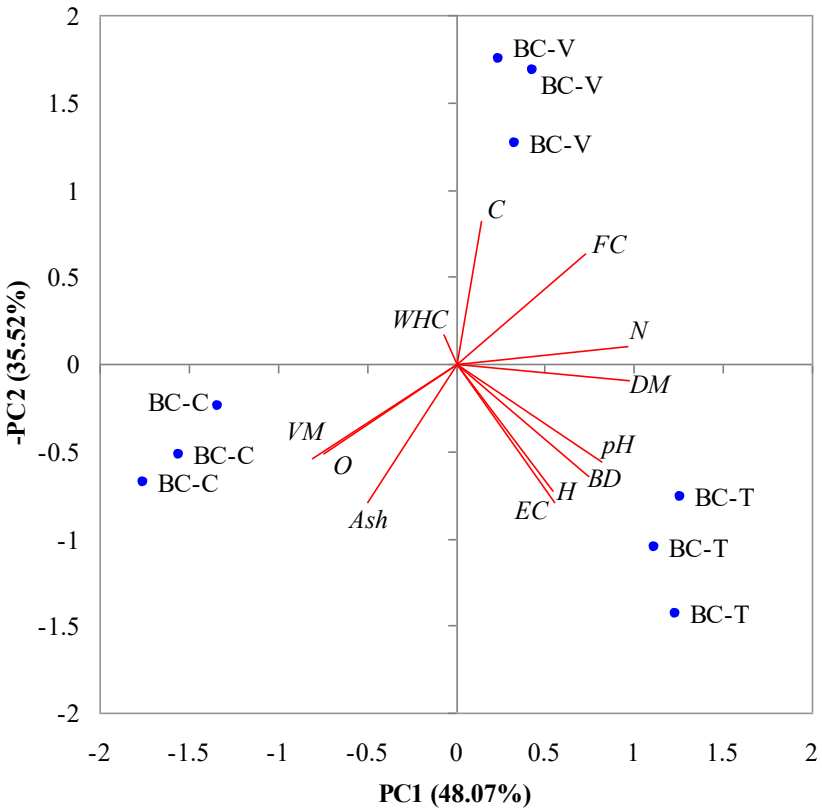


Figure 32. Projections of variables (*DM, VM, Ash, FC, C, H, N, O, BD, EC, pH,* and *WHC*) and samples (BC-V, BC-T, and BC-C) on the PC1–PC2 plane.

The projections of the variables (*DM, VM, Ash, FC, C, H, N, O, BD, EC, pH,* and *WHC*) and the samples (BC-V, BC-T, and BC-C) on the PC1–PC2 plane (Figure 32) indicate the following: (i) the biochar derived from grape pomace (BC-T) shows higher levels of dry matter content (*DM*), fixed carbon (*FC*), nitrogen concentration (*N*), bulk density (*BD*), and *pH*, but lower levels of volatile matter content (*VM*) and oxygen concentration (*O*), compared to the biochar obtained from chrysanthemum residues (BC-C). This differentiation is reflected in their positions on PC1, where BC-T has positive coordinates and BC-C has negative ones; (ii) the biochar produced from vine prunings (BC-V) exhibits higher carbon concentration (*C*), but lower electrical conductivity (*EC*), ash content (*Ash*), and hydrogen concentration (*H*) relative to BC-T. This contrast is observed on PC2, with BC-V having positive coordinates and BC-T negative; (iii) Statistically significant positive correlations were identified between the following variable pairs: *DM* and *N, DM* and *BD, DM* and *pH, VM* and *Ash, VM* and *O, Ash* and *O, FC* and *N, H* and *BD, H* and *EC, H* and *pH, N* and *BD, N* and *pH, BD* and *EC, BD* and *pH,* and *EC* and *pH;* (iv) Statistically significant negative correlations were found between the following variable pairs: *DM* and *VM, DM* and *O, VM* and *FC, VM* and *N, Ash* and *FC, FC* and *O, C* and *O,* and *N* and *O.*

Table 25. Coordinates of variables on factors PC1 and PC2 for biochar samples obtained from vine prunings (BC-V), grape pomace (BC-T), and chrysanthemum residues (BC-C).

No.	Variable symbol	PC1	PC2
1	*Ca*	-0.425	**0.904**
2	*P*	0.246	**0.969**
3	*K*	**0.789**	-0.591
4	*Zn*	**-0.998**	0.063
5	*Al*	**1.000**	-0.022
6	*B*	**0.768**	0.640
7	*Cu*	**0.765**	0.644
8	*Fe*	**0.910**	0.415
9	*Mg*	-0.635	**0.771**
10	*Mn*	**0.883**	0.470
11	*Co*	**0.936**	-0.352
12	*Mo*	**-0.963**	0.269

Significant values are highlighted in bold.

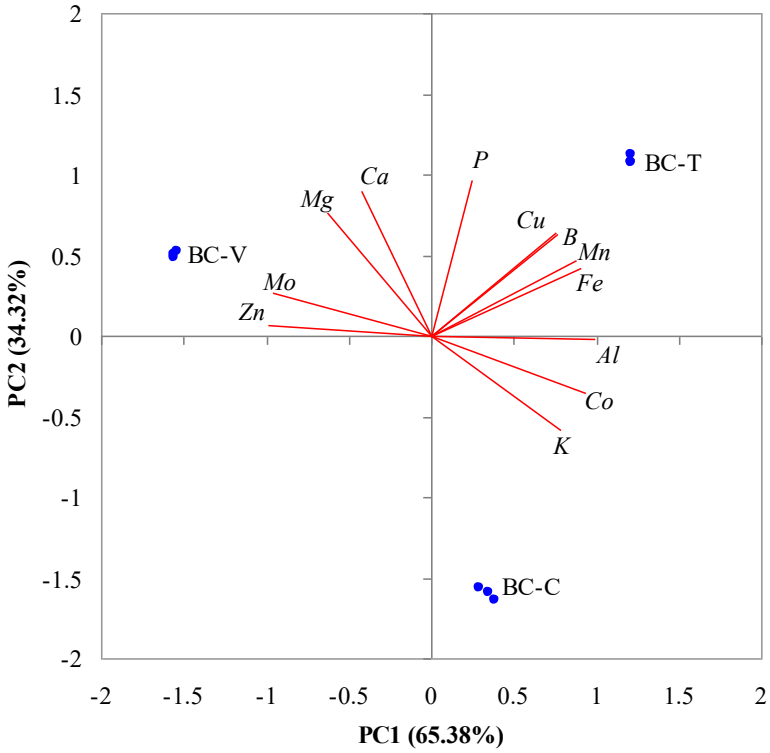


Figure 33. Projections of variables (*Ca, P, K, Zn, Al, B, Cu, Fe, Mg, Mn, Co,* and *Mo*) and samples (BC-V, BC-T, and BC-C) on the PC1–PC2 plane.

The projections of the variables (*Ca, P, K, Zn, Al, B, Cu, Fe, Mg, Mn, Co,* and *Mo*) and the samples (BC-V, BC-T, and BC-C) on the PC1–PC2 plane (Figure 33) indicate the following aspects: (i) the biochars produced from grape pomace (BC-T) and chrysanthemum residues (BC-C) show higher concentrations of potassium (*K*), iron (*Fe*), aluminum (*Al*), boron (*B*), manganese (*Mn*), copper (*Cu*), and cobalt (*Co*), but lower concentrations of zinc (*Zn*) and molybdenum (*Mo*), compared to the biochars derived from vine prunings (BC-V). This is reflected in the discrimination on PC1, where BC-T and BC-C have positive coordinates, while BC-V has negative ones; (ii) The biochars obtained from vine prunings (BC-V) and grape pomace (BC-T) display higher levels of calcium (*Ca*), phosphorus (*P*), and magnesium (*Mg*), relative to the one derived from chrysanthemum residues (BC-C), which is differentiated along

PC2 with BC-V and BC-T showing positive coordinates and BC-C negative; (iii) Statistically significant positive correlations were identified among: *Ca* and *P, Ca* and *Mn, P* and *B, P* and *Cu, P* and *Mn, K* and *Al, K* and *Co, Zn* and *Mg, Zn* and *Mo, Al* and *B, Al* and *Cu, Al* and *Fe, Al* and *Mn, Al* and *Co, B* and *Cu, B* and *Fe, B* and *Mn, Cu* and *Fe, Cu* and *Mn, Fe* and *Mn, Fe* and *Co,* and *Mg* and *Mo;* (iv) Statistically significant negative correlations were found between: *Ca* and *K, Ca* and *Co, K* and *Zn, K* and *Mg, K* and *Mo, Zn* and *Al, Zn* and *B, Zn* and *Cu, Zn* and *Fe, Zn* and *Mn, Zn* and *Co, Al* and *Mo, Fe* and *Mo, Mg* and *Co, Mn* and *Mo,* and *Co* and *Mo.*

Furthermore, from the projections of the variables (*Ca, P, K, Zn, Al, B, Cu, Fe, Mg, Mn, Co,* and *Mo*) and samples related to plant residues and biochar (Figure 33), the following patterns are observed: (i) the plant residue (V) and corresponding biochar (BC-V) show higher magnesium (*Mg*) concentrations compared to T, C, BC-T, and BC-C; (ii) the grape pomace (T) and its biochar (BC-T) exhibit higher concentrations of potassium (*K*), boron (*B*), and copper (*Cu*) compared to V, C, BC-V, and BC-C; (iii) the chrysanthemum residues (C) and corresponding biochar (BC-C) have higher concentrations of aluminum (*Al*), cobalt (*Co*), iron (*Fe*), and manganese (*Mn*) relative to V, T, BC-V, and BC-T.

2.1.1.3. Conclusions

Slow pyrolysis of residual plant materials—i.e., vine prunings, grape pomace, and chrysanthemum residues—was carried out for 1 hour in a fixed-bed reactor, using CO_2 as both carrier gas and mild oxidizing agent. Biochar, bio-oil, and pyrolytic gases were produced under various operating conditions.

A detailed experimental study based on a 2^3 factorial design was conducted for the pyrolysis of shredded vine prunings. The independent process variables (factors) were heat flux (q = 4244−5777 W/m²), superficial CO_2 velocity (w = 0.004−0.008 m/s), and the mean particle diameter of biomass (d = 0.007–0.011 m). The specific yields of the solid and liquid phases—defined as the mass of pyrolytic product divided by the initial mass of biomass—and the average temperature of the fixed bed were selected as dependent variables (responses). The final specific yields of biochar and bio-oil ranged from 0.286 to 0.328 and from 0.260 to 0.350, respectively, while the average bed temperature ranged between 401.1 and 486.5 °C.

Multiple regression equations were obtained relating the dimensionless factors ((x_1, x_2 and x_3) to the final values of the process responses. Under the studied conditions, the effects of heat flux (x_1), carrier gas velocity (x_2), and biomass particle size (x_3) on the final pyrolysis performance were as follows:

- x_2 had a significant positive effect and x_3 a significant negative effect on biochar yield;
- x_3 had a significant positive effect, while x_1x_2, x_1x_3 and $x_1x_2x_3$ showed negative effects on bio-oil yield;
- x_2 had a significant negative effect, x_3 a significant positive effect, and both x_1x_3 and x_2x_3 had significant positive effects on the average bed temperature.

The plant materials and the resulting biochar were characterized using specific analytical methods. Due to the low bulk density (0.112 ± 0.001 g/cm³) and electrical conductivity (0.55 ± 0.03 dS/m), as well as relatively high pH (10.35 ± 0.06), water-holding capacity (58.99 ± 14.51%), and concentrations of phosphorus (6.142 ± 0.093 mg/g), calcium (14.52 ± 0.12 mg/g), and magnesium (2.632 ± 0.026 mg/g), the biochar derived from vine prunings could be recommended as a soil amendment for acidic soils. Furthermore, its structure can be modified by impregnating the raw material with acidic or basic solutions, enabling the production of tailored biochar for specific applications, e.g., environmental remediation.

2.1.2. PRODUCTION, CHARACTERIZATION, AND TESTING OF MODIFIED (ACTIVATED) BIOCHAR AS AN ADSORBENT BY IMPREGNATING THE RAW MATERIAL WITH ALKALINE OR ACIDIC SOLUTIONS

2.1.2.2. Production and testing of biochar and activated biochar as adsorbents by impregnating the raw material with phosphoric acid (H_3PO_4) solutions

2.1.2.2.1. Pretreatment of plant material

The vine prunings, cut into cylindrical pieces, were impregnated with H_3PO_4 solutions of different concentrations, i.e., 10%, 31%, 48%, and 52%. The impregnation ratio (*IR*), defined by equation (16), where m_acid and m_residue represent the masses of H_3PO_4 and vine residue, respectively, was 0.3 g/g, 1.1 g/g, 1.9 g/g, and 2.2 g/g. Impregnations were carried out in perfectly stirred reactors for 2 hours, after which the solid-liquid suspensions were filtered and the impregnated material was dried in an oven for 12 hours (Figure 43).

$$IR = \frac{m_{acid}}{m_{rez}} \tag{16}$$

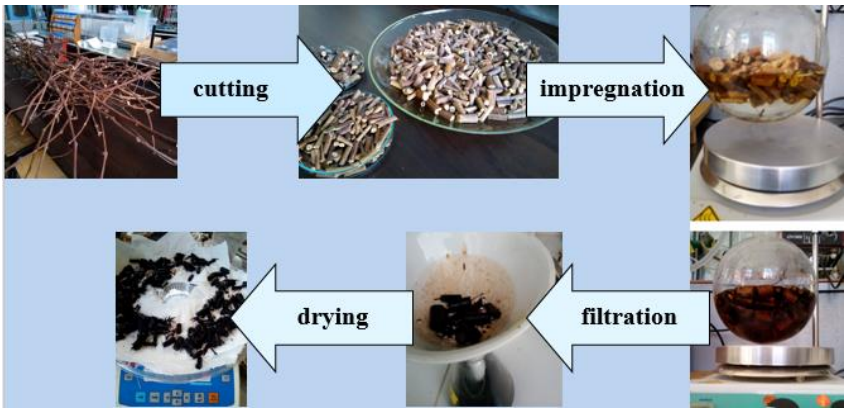


Figure 43. Scheme of main operations for the pretreatment of vine pruning residues.(Calcan et al., 2025).

2.1.2.2.2. Production of biochar (BC)/activated biochar (ABC) by slow pyrolysis of unimpregnated/impregnated plant material

Unimpregnated and impregnated shredded vine residues were pyrolyzed in a laboratory-scale pilot plant, resulting in biochar (BC) and activated biochar (ABC). Slow pyrolysis of the plant material was conducted in the presence of CO_2, used as a carrier gas and reactant. Following a two-factor central composite design (CCD) experimental plan, 12 experimental tests were performed. The heat flux (q = 4.3–6.6 kW/m²) and the impregnation ratio (*IR* = 0.0–2.2 g/g) were selected as the process factors for pyrolysis.

Table 33. Experimental values of pyrolysis and adsorption process responses at different levels of dimensional and dimensionless factors.

Exp.	q (kW/m^2)	IR (g/g)	x_1	x_2	m_f/m_0 (g/g)	m_{Lf}/m_0 (g/g)	t_{mf} (°C)	$C_{if,ads}$ (g/g)
1	4.6	0.3	-1	-1	0.410	0.250	352	0.077
2	4.6	1.9	-1	1	0.522	0.230	360	0.112
3	6.2	0.3	1	-1	0.354	0.300	404	0.103
4	6.2	1.9	1	1	0.430	0.280	417	0.134
5	5.4	1.1	0	0	0.530	0.260	382	0.110
6	5.4	1.1	0	0	0.542	0.265	383	0.102
7	4.3	1.1	-1.414	0	0.481	0.237	345	0.093
8	6.6	1.1	1.414	0	0.377	0.334	422	0.136
9	5.4	0.0	0	-1.414	0.310	0.308	416	0.064
10	5.4	2.2	0	1.414	0.495	0.260	370	0.110
11	5.4	1.1	0	0	0.528	0.261	380	0.102
12	5.4	1.1	0	0	0.537	0.272	381	0.108
Valoare minimă (*MIN*)					0.310	0.230	345	0.064
Valoare maximă (*MAX*)					0.542	0.334	422	0.136
Valoare medie					0.460	0.271	384	0.104
Abatere standard (*SD*)					0.081	0.030	25.8	0.020

$$x_1 = \frac{q - 5{,}4}{0{,}8} \quad (17) \qquad x_2 = \frac{IR - 1{,}1}{0{,}8} \quad (18)$$

The levels of the dimensional factors (q and IR) and those of the dimensionless factors (x_1 and x_2), as defined by equations (17) and (18), are specified in Table 33. The final values (f) (at τ_f =60 min) of the specific solid phase yield (BC/ABC), m_f/m_0 - where m_0 (g) represent the initial mass of the unimpregnated/impregnated biomass residues—the specific liquid phase yield (pyrolytic oil), m_{Lf}/m_0, and the logarithmic mean temperature of the fixed biomass bed, t_{mf}, as defined by equation (2), were selected as the dependent variables (responses) of the pyrolysis process.

2.1.2.2.3. Testing BC and ABC as adsorbents for volatile organic compounds (VOCs)

BC and ABC obtained by slow pyrolysis of unimpregnated and impregnated vine residues (experiments 1–12 in Table 33) were tested as adsorbents for 1,2-dichloroethane (DCE) from an air stream. DCE is a VOC with a boiling point of 83.5 °C at atmospheric pressure and a vapor pressure of 7.7 kPa at 20 °C.

A part of the adsorption setup is shown in Fig. 45. BC/ABC was packed into the glass column (1), 1.7 cm internal diameter and 29 cm height, which was placed in the holder (2) and put on the digital balance (3) in an enclosure with insulating polystyrene walls (4). A compressor fed air into the silica gel column (5) to remove the humidity and further bubbled into the liquid VOC species from a bubbler. The mixture of air and VOC vapour exiting the bubbler was introduced into the adsorption column (1) and passed upward through the BC/ABC fixed bed until it was saturated. The finned heater (6) increased the temperature inside the insulating enclosure and maintained it at a constant value. The thermal agent in the heater (6) was warm water from the thermostatic bath (7). The amount of adsorbed VOC was estimated based on the increase in the mass of the adsorption column, considering that the saturation state was attained when the column mass did not vary for 10 min.

Twelve adsorption experimental runs were performed for 90 min at 40 °C, 1 atm, and a level of air superficial velocity of 0.7 cm/s. Final (f) values (at $\tau_{f,ads}$ = 90 min) of BC/ABC adsorption capacity for i species of VOC ($C_{if,ads}$) defined by Eq. (6), where $m_{if,ads}$ (g) represents

the mass of *i* species (DCE) adsorbed at $\tau_{f,ads}$ and $m_{BC/ABC,0}$ (g) the initial mass of BC/ABC, was selected as response of adsorption process.

$$C_{if,ads} = \frac{m_{if,ads}}{m_{BC/ABC,0}} \quad (19)$$



Figure 45. Adsorption setup: (1) glass adsorption column; (2) holder; (3) digital balance; (4) insulating enclosure; (5) silica gel column; (6) finned heater; (7) water bath.

The experimental values of the responses obtained at different levels of the pyrolysis process factors were processed using CCD. Statistical analysis was performed using STATISTICA version 10.0 (StatSoft Inc., Tulsa, OK, USA).

Experimental values of pyrolysis and adsorption process responses at different levels of factors are summarized in Table 33. It is observed that maximum values of m_{Lf}/m_0, t_{mf}, and $C_{if,ads}$ were obtained in exp. 8 (q = 6.6 kW/m^2 and IR = 1.1 g/g, corresponding to x_1 = 1.414 and x_2 = 0), whereas minimum values of m_L/m_0 and $C_{if,ads}$ were obtained in exp. 9 (q = 5.4 kW/m^2 and IR = 0, corresponding to x_1 = 0 and x_2 = -1.414). Correlation analysis indicated a very strong positive correlation between m_{Lf}/m_0 and t_{mf} responses (r = 0.9) as well as strong negative correlations between m_f/m_0 and m_{Lf}/m_0 (r = -0.7) and m_f/m_0 and t_{mf} (r = -0.6), consistent with previous results (Calcan et al., 2022a, Dobre et al., 2012, Pârvulescu et al., 2011).

The effects of x_1, x_1^2, x_2, x_2^2 and x_1x_2 on y_j (j = 1…4) were quantified using second-order polynomial models expressed by equation (20), where $y_1 = (m_f/m_0)_{calc}$, $y_2 = (m_{Lf}/m_0)_{calc}$, $y_3 = t_{mf,calc}$ and $y_4 = C_{if,ads,calc}$ represent the calculated responses, and β_{kj} (k = 1…6, j = 1…4) are the regression coefficients (Figures 46-49).

$$y_j = \beta_{1j} + \beta_{2j}x_1 + \beta_{3j}x_1^2 + \beta_{4j}x_2 + \beta_{5j}x_2^2 + \beta_{6j}x_1x_2, j = 1\ldots4 \quad (20)$$

Table 34. Regression coefficients (β_{kj}, $k = 1…6$, $j = 1…4$) in Eq. (6) and related p-values (p_{kj}), multiple determination coefficient (R^2), adjusted R^2 (R^2_{adj}), residual standard error (RSE), F statistic (F), and p-value for F (p).

j		1		2		3		4	
Response		$y_1 = (m_f/m_0)_{calc}$		$y_2 = (m_{Lf}/m_0)_{calc}$		$y_3 = t_{mf,calc}$		$y_4 = C_{if,ads,calc}$	
Regressor	k	β_{k1}	p_{k1}	β_{k2}	p_{k2}	β_{k3}	p_{k3}	β_{k4}	p_{k4}
Intercept	1	**0.534**	0.0000	**0.265**	0.0000	**381.5**	0.0000	**0.105**	0.0000
x_1	2	**-0.037**	0.0003	**0.030**	0.0009	**27.24**	0.0009	**0.014**	0.0002
x_1^2	3	**-0.049**	0.0001	0.006	0.3468	-0.251	0.9620	**0.006**	0.0202
x_2	4	**0.056**	0.0000	**-0.013**	0.0325	-5.506	0.2689	**0.016**	0.0001
x_2^2	5	**-0.063**	0.0000	0.005	0.4112	4.500	0.4076	**-0.008**	0.0062
$x_1 x_2$	6	-0.009	0.2423	0.000	1.0000	1.250	0.8514	-0.001	0.6909
R^2		0.984		0.885		0.866		0.970	
R^2_{adj}		0.970		0.789		0.754		0.944	
RSE		0.014		0.014		12.79		0.005	
F		73.24		9.241		7.735		38.29	
p		0.000		0.009		0.014		0.000	

Statistically significant coefficients ($p_{kj} \leq \alpha = 0.05$, where α is the significance level) are written in bold.

Table 35. Predicted values of pyrolysis and adsorption responses at different levels of dimensionless factors

Exp.	x_1	x_2	y_1 (g/g)	y_2 (g/g)	y_3 (°C)	y_4 (g/g)
1	-1	-1	0.394	0.259	365	0.073
2	-1	1	0.524	0.232	352	0.107
3	1	-1	0.338	0.318	417	0.102
4	1	1	0.433	0.291	409	0.133
5	0	0	0.534	0.265	382	0.105
6	0	0	0.534	0.265	382	0.105
7	-1.414	0	0.488	0.234	342	0.098
8	1.414	0	0.383	0.318	420	0.137
9	0	-1.414	0.330	0.293	398	0.067
10	0	1.414	0.489	0.255	383	0.113
11	0	0	0.534	0.265	382	0.105
12	0	0	0.534	0.265	382	0.105
Minimum value (*MIN*)			0.330	0.232	342	0.067
Maximum value (*MAX*)			0.534	0.318	420	0.137
Mean value			0.460	0.271	384	0.104
Standad deviation (*SD*)			0.080	0.028	24.0	0.020

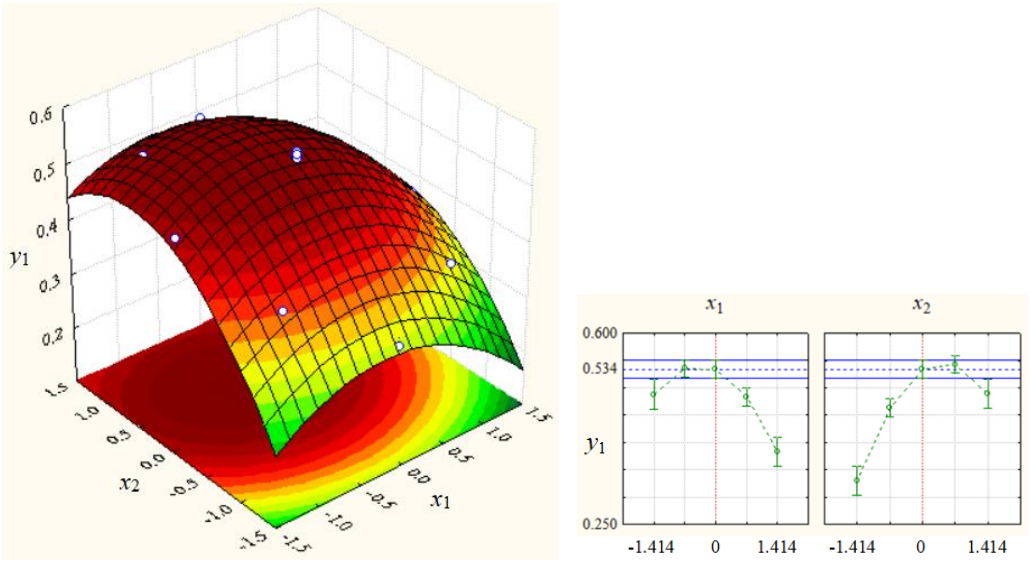


Figure 46. Effects of dimensionless factors on $y_1 = (m_f/m_0)_{calc}$ (Calcan et al., 2025).

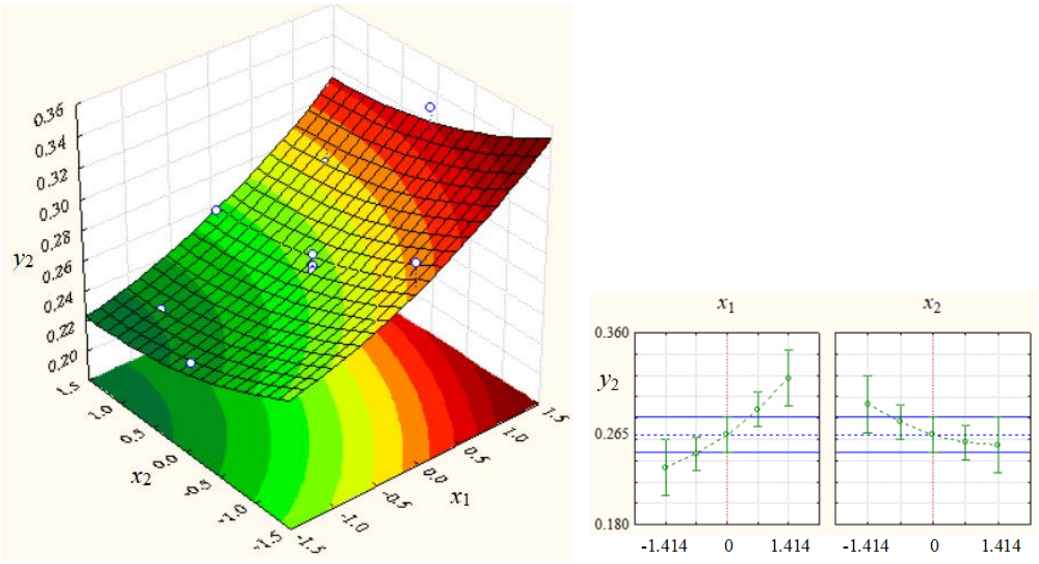


Figure 47. Effects of dimensionless factors on $y_2 = (m_{Lf}/m_0)_{calc}$ (Calcan et al., 2025).

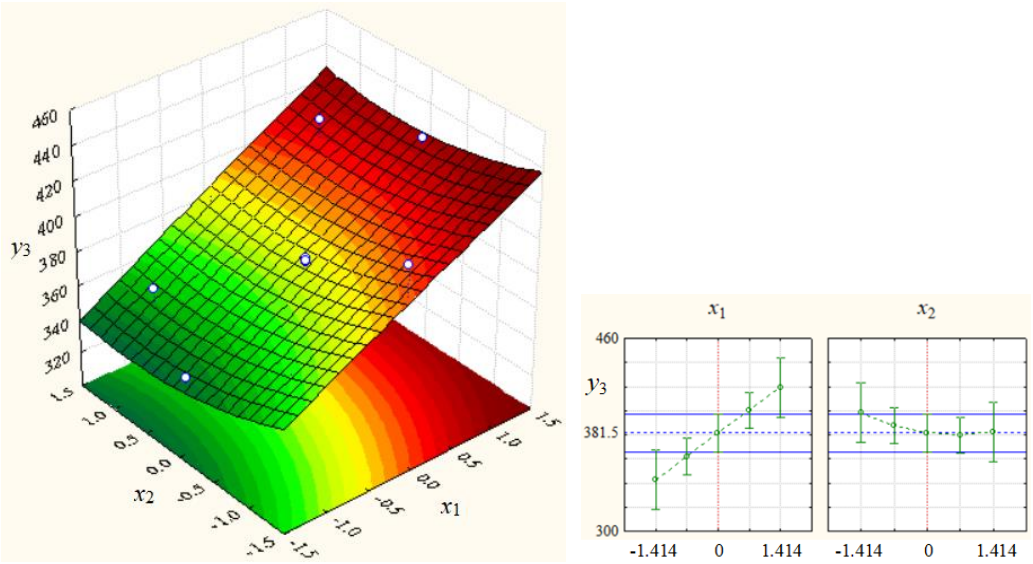


Figure 48. Effects of dimensionless factors on $y_3 = t_{mf,calc}$ (Calcan et al., 2025).

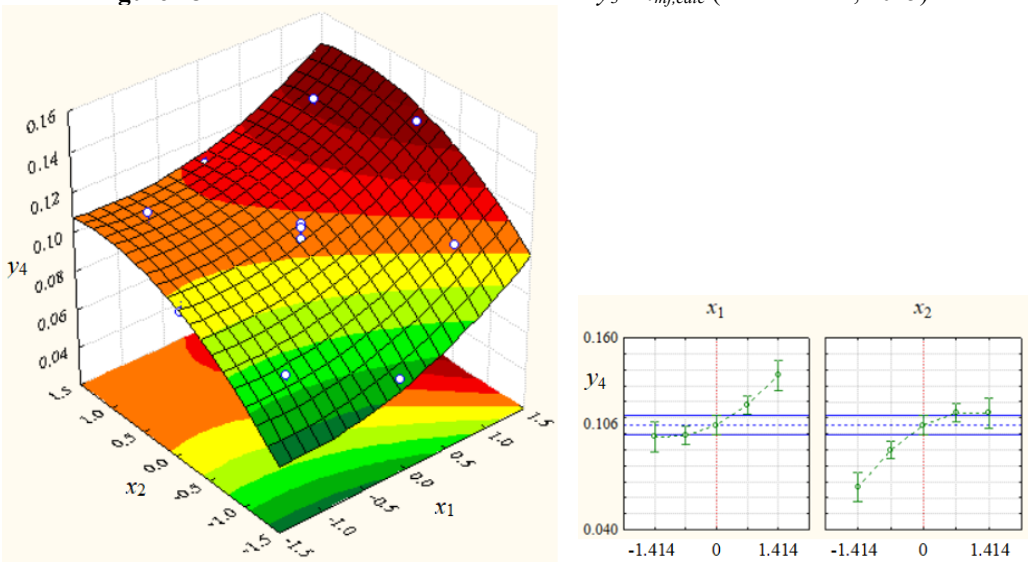


Figure 49. Effects of dimensionless factors on $y_4 = C_{if,ads,calc}$ (Calcan et al., 2025).

2.1.2.3. Conclusions

The production of biochar (BC) and chemically modified biochar (ABC) from vine pruning residues, which are often burned, and the application of BC/ABC as VOC adsorbents can have significant environmental and economic benefits.

Pyrolysis factors in terms of heat flux (q = 4.3–6.6 kW/m^2) and impregnation ratio (IR = 0–2.2 g/g) affected pyrolysis and adsorption performances as follows: (i) specific mass of BC/ABC (m_f/m_0 = 0.310–0.542) decreased significantly as q increased from 5.4 kW/m^2 to 6.6 kW/m^2 and IR decreased from 1.1 g/g to 0 (no impregnation); (ii) q had a significant positive effect on specific mass of bio-oil (m_{Lf}/m_0 = 0.230–0.334 g/g) and mean temperature of BC/ABC bed (t_{mf} = 345–422 °C); (iii) BC/ABC adsorption capacity for DCE ($C_{if,ads}$ = 0.064–0.136 g/g) increased with an increase in q and IR, the increase being significant for q = 5.4–6.6 kW/m^2 and IR = 0–1.1 g/g. Moreover, m_{Lf}/m_0 and t_{mf} were very strongly positively correlated, whereas m_f/m_0 and m_{Lf}/m_0 as well as m_f/m_0 and t_m were strongly negatively correlated.

The effects of q and IR on selected responses were quantified using second-order polynomial models. Maximum predicted values of adsorption capacity (0.137 g/g), specific mass of bio-oil (0.318 g/g), and mean temperature of BC/ABC bed (420 °C) were obtained at q = 6.6 kW/m^2 and IR = 1.1 g/g.

2.2. SLOW PYROLYSIS OF AGRO-INDUSTRIAL RESIDUES IN A LABORATORY-SCALE PILOT INSTALLATION

2.2.1.PRODUCTION OF BIOCHAR

2.2.1.1. Materials, equipment, and methods

Slow pyrolysis of vine pruning residue was performed at the University POLITEHNICA of Bucharest (UPB) Department of Chemical and Biochemical Engineering, using a laboratory-scale pilot experimental installation (Figure 51), the relevants parameters are presented in Table 36.

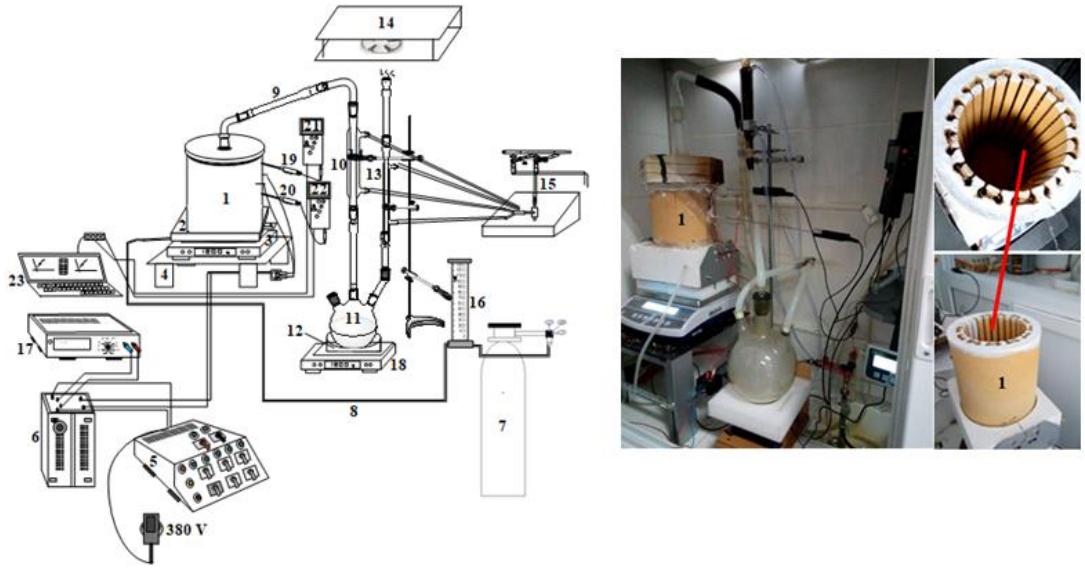


Figure 51. Experimental setup: (1) pyrolysis reactor; (2) ACC support; (3) precision balance (max. 30 kg); (4) metal support; (5), (6) power transformers; (7) gas tank; (8) sweeping gas feed pipe; (9) pipe collecting volatile products; (10), (13) double pipe heat exchangers; (11) oil collector; (12) PU Figure 2. Experimental setup: (1) pyrolysis reactor; (2) ACC support; (3) precision balance (max. 30 kg); (4) metal support; (5), (6) power transformers; (7) gas tank; (8) sweeping gas feed pipe; (9) pipe collecting volatile products; (10), (13) double pipe heat exchangers; (11) oil collector; (12) PU support; (14) exhaust hood; (15) coolant supply/discharge system; (16) flow meter; (17) voltmeter; (18) precision balance (max. 10 kg); (19), (20) thermocouples; (21), (22)

thermometers; (23) data recording and processing system. support; (14) exhaust hood; (15) coolant supply/discharge system; (16) flow meter; (17) voltmeter; (18) precision balance (max. 10 kg); (19), (20) thermocouples; (21), (22) thermometers; (23) data recording and processing system (Calcan et al., 2022b).

Table 36. Relevant parameters of the furnace (Figure 51) and the pyrolysis column (Figure 15).

No.	Parameter (unit)	Furnace	Column
1	Height (cm)	27	50
2	Inner diameter (cm)	15.5	3
3	Wall thickness (cm)	3.5	0.4
4	Internal cross-sectional area (cm^2)	188.7	7.1
5	Internal volume (cm^3)	5094.7	353.4
6	Initial height of the vegetable material bed (cm)	24	30
7	Initial volume of the vegetable material bed (cm^3)	4528.6	212.1

2.2.2. CHARACTERIZATION AND APPLICATION OF BIOCHAR AS A SOIL AMENDMENT

2.2.2.1. Materials, equipment, and methods

2.2.2.1.1. Soil amendment with biochar

Three types of clay soils (Table 37) were ground using a soil mill and amended with highly alkaline biochar (pH = 9.89 ± 0.01), which had been previously ground. The soil (S) to biochar (BC) mixing ratio was 4:1 v/v.

Table 37. Types of soils amended with biochar

Soil type	Symbol	pH	Character	Sampling location
Calcareous alluvial soil	S1	7.99 ±	Slightly	Grădiștea Commune (Călărași
Typical vermic	S2	6.26 ±	Slightly acidic	Perișoru Commune (Călărași County)
Typical luvic soil	S3	5.40 ±	Strongly acidic	Albota Commune (Argeș County)

2.2.2.1.2. Characterization of soils, biochar (BC), and BC-amended soils

The soils, BC, and soil + BC mixtures were analyzed at the Research Center for the Study of Agri-Food Product Quality (USAMV). The following parameters were determined: humidity (*HU*), bulk density (*BD*), concentrations of soluble nitrate nitrogen (*N-NO_3*), soluble ammonium nitrogen (*N-NH_4*), soluble phosphorus (*P*), soluble potassium (*K*), mobile phosphorus and potassium concentrations (*P-AL* and *K-AL*), concentrations of *Ca, Mg,* and *Na*, and total carbon (*C*) content.

2.2.2.1.3. Greenhouse Experiment

A greenhouse experiment was conducted over 66 days to evaluate the effects of biochar (BC) application on tomato plant growth. The plants were cultivated in the greenhouse of the Research Center for the Study of Food Quality Products (USAMV). According to the experimental design shown in Table 38, five treatments were applied for each soil type.

Table 38. Treatments used in the greenhouse experiment (Calcan et al., 2022b; Egri et al., 2022)

No.	**Treatment**	**Code**
1	No BC and foliar fertilizer treatments	S
2	BC(volumetric ratio between BC and soil of 20/80)	S + BC
3	Foliar fertilizer (0.2%)	S + F
4	BC + foliar fertilizer (0.2%)	S + BC + F
5	BC + foliar fertilizer (0.1%)	S + BC + F/2

Plant height (*H*), number of leaves (*NL*), collar diameter (*CD*), and root volume (*RV*), evaluated 66 days after sowing, were selected as dependent variables.

2.2.2.2. Results and discussion

2.2.2.2.1. Characterization of soils, biochar (BC), and soils amended with BC

The average values of the physico-chemical properties of the soils (S1, S2, and S3), the biochar (BC), and the soils amended with BC (S1 + BC, S2 + BC, and S3 + BC) are presented in Table 39.

Table 39. Average values of the physico-chemical properties of the soils (S), biochar (BC), and BC-amended soils (S + BC) (Calcan et al., 2022b).

Nr.	Property	S1	S2	S3	BC	S1 + BC	S2 + BC	S3 + BC
1	*HU* (%)	14.69	10.43	13.10	3.506	12.33	9.596	12.36
2	*BD* (g/cm^3)	1.054	0.986	1.314	0.319	0.799	0.851	0.873
3	*pH*	7.989	6.258	5.403	9.894	8.334	7.095	6.445
4	*EC* (dS/m)	0.217	0.095	0.094	2.044	0.345	0.208	0.158
5	*C* (%)	2.888	2.006	1.981	76.01	10.99	10.26	14.35
6	*N-NO*$_3$ (mg/kg)	31.24	14.89	9.232	5.411	26.17	11.26	8.038
7	*N-NH*$_4$ (mg/kg)	11.90	11.32	2.969	15.63	13.86	12.41	3.737
8	*P* (mg/kg)	6.337	2.251	0.768	16.03	13.58	14.69	2.901
9	*K* (mg/kg)	23.89	5.521	6.409	3131	132.0	130.1	51.12
10	*P-AL* (mg/kg)	103.6	16.41	12.65	1615	226.7	168.7	86.67
11	*K-AL* (mg/kg)	360.0	200.0	240.0	8200	1040	860.0	700.0
12	*Ca* (mg/kg)	2990	2940	2366	2044	2763	2443	2202
13	*Mg* (mg/kg)	371.9	308.3	605.9	472.2	386.6	334..4	582.7
14	*Na* (mg/kg)	31.09	31.03	44.89	87.94	35.28	34.68	50.53

(HU) humidity, (BD) bulk density, (EC) electrical conductivity, (C) total carbon concentration, (N-NO_3) soluble nitrate nitrogen concentration, (N-NH_4) soluble ammonium nitrogen concentration, (P) soluble phosphorus concentration, (K) soluble potassium concentration, (P-AL) mobile phosphorus concentration, (K-AL) mobile potassium concentration, (Ca) mobile calcium concentration, (Mg) mobile magnesium concentration, (Na) mobile sodium concentration.

Data presented in Table 39 indicate the following issues:

(i) the values of humidity (*HU*), bulk density (*BD*), soluble N-NO_3 content (*N-NO*$_3$), and available Ca content (*Ca*) are higher for soils than for BC (3-4 times for *HU* and *BD*, 2-6 times for *N-NO*$_3$, 16-46% for *Ca*) and BC-amended soils (6-19% for *HU*, 16-50% for *BD*, 15-32% for *N-NO*$_3$, 7-20% for *Ca*);

(ii) the values of *pH*, electrical conductivity (*EC*), total carbon content (*C*), concentrations of soluble N-NH_4 (*N-NH*$_4$), soluble P and K (*P* and *K*), available P and K (*P-LA* and *K-LA*), and available Na (*Na*) are lower for soils than for BC (24-83% for *pH*, 9-22 times for *EC*, 26-38 times for *C*, up to 5 times for *N-NH*$_4$, 3-21 times for *P*, 131-567 times for *K*, 16-128 times for *P-LA*, 23-41 times for *K-LA*, and 2-3 times for *Na*) and BC-amended soils (4-19% for *pH*, about 2 times for *EC*, 4-7 times for *C*, 10-26% for *N-NH*$_4$, 2-7 times for *P*, 6-24 times for *K*, 2-10 times for *P-LA*, 3-4 times for *K-LA*, and up to 13% for *Na*);

(iii) the values of available Mg content (*Mg*) are higher for soil 3 than for BC (by 28%) and soil 3+BC mixture (by 4%), whereas the values of *Mg* are lower for soils 1 and 2 than for BC (up to 53%) as well as for soil 1+BC and soil 2+BC mixtures (up to 8%).

The results presented in Figure 52 and Tables 40–42 highlight the following relevant issues:

(i) BC has higher levels of *C* (76.01±0.68%), *EC* (2.044±0.070 dS/m), *pH* (9.89±0.01), *K-LA* (8200±0.00 mg/kg), *P-LA* (1615±7.25 mg/kg), *K* (3131±183 mg/kg), *P* (16.03±0.28 mg/kg), and *Na* (87.94±5.97 mg/kg), but lower levels of *BD* (0.319±0.018 g/cm^3) and *HU* (3.51±0.18%) than other samples [discrimination on PC1 between BC (blue circle) and the other samples];

(ii) soil 3 and soil 3+BC mixture have higher levels of *Mg* (572.2-607.5 mg/kg) and lower levels of *N-NO*$_3$ (8.04-9.65 mg/kg), *N-NH*$_4$ (2.82-4.05 mg/kg), and *Ca* (2182-2373 mg/kg) than the other non-amended and BC-amended soils (*Mg*=302.6-388.1 mg/kg, *N-NO*$_3$=10.55-32.82 mg/kg, *N-NH*$_4$=11.02-14.05 mg/kg, and *Ca*=2415-3035 mg/kg) [discrimination on PC2 between soil 3 and soil 3+BC mixture and the other non-amended and BC-amended soils (green circles)];

(iii) *pH*, *EC*, *C*, *N-NH*$_4$, *P*, *K*, *P-LA*, *K-LA*, and *Na* are directly correlated, and they are inversely correlated with *HU*, *BD*, *N-NO*$_3$, and *Ca*;

(iv) there are very strong positive correlations ($r \geq 0.85$) between *EC* and *C* (r=0.97), *Na* and *C* (r=0.94), *Na* and *EC* (r=0.88);

(v) there are very strong negative correlations between *BD* and *C* (r=-0.89), *HU* and *K-LA* (r=-0.87), *BD* and *EC* (r=-0.86), *BD* and *pH* (r=-0.85).

The data were analyzed using principal component analysis (PCA).

Table 40. Coordinates of variables projections on the axes on the axes PC1 and PC2 (Calcan et al., 2022b).

Variable	PC1	PC2
HU	**-0.778**	-0.061
BD	**-0.927**	0.202
pH	**0.818**	-0.459
EC	**0.958**	0.007
C	**0.985**	0.117
N-NO$_3$	-0.283	**-0.721**
N-NH$_4$	0.477	**-0.812**
P	**0.703**	-0.333
K	**0.810**	0.005
P-LA	**0.805**	0.000
K-LA	**0.848**	0.053
Ca	-0.468	**-0.773**
Mg	0.044	**0.875**
Na	**0.884**	0.410

Table 41. Coordinates of samples projection on the axes PC1 and PC2 (Calcan et al., 2022b).

Sample	PC1	PC2
1	-1.298	-1.423
1	-1.886	-2.169
1	-1.574	-1.750
2	-1.627	-1.040
2	-1.711	-0.929
2	-1.582	-1.294
3	-2.606	**2.800**
3	-2.501	**2.746**
3	-1.773	**2.692**
1 + BC	-0.303	-1.572
1 + BC	-0.174	-2.060
1 + BC	-0.260	-1.860
2 + BC	0.165	-0.644
2 + BC	-0.093	-0.785
2 + BC	-0.289	-0.879
3 + BC	-0.998	**2.607**
3 + BC	-0.701	**2.352**
3 + BC	-0.553	**1.923**
BC	**6.606**	0.856
BC	**7.072**	0.433
BC	**6.084**	-0.005

Significant values are highlighted in bold.

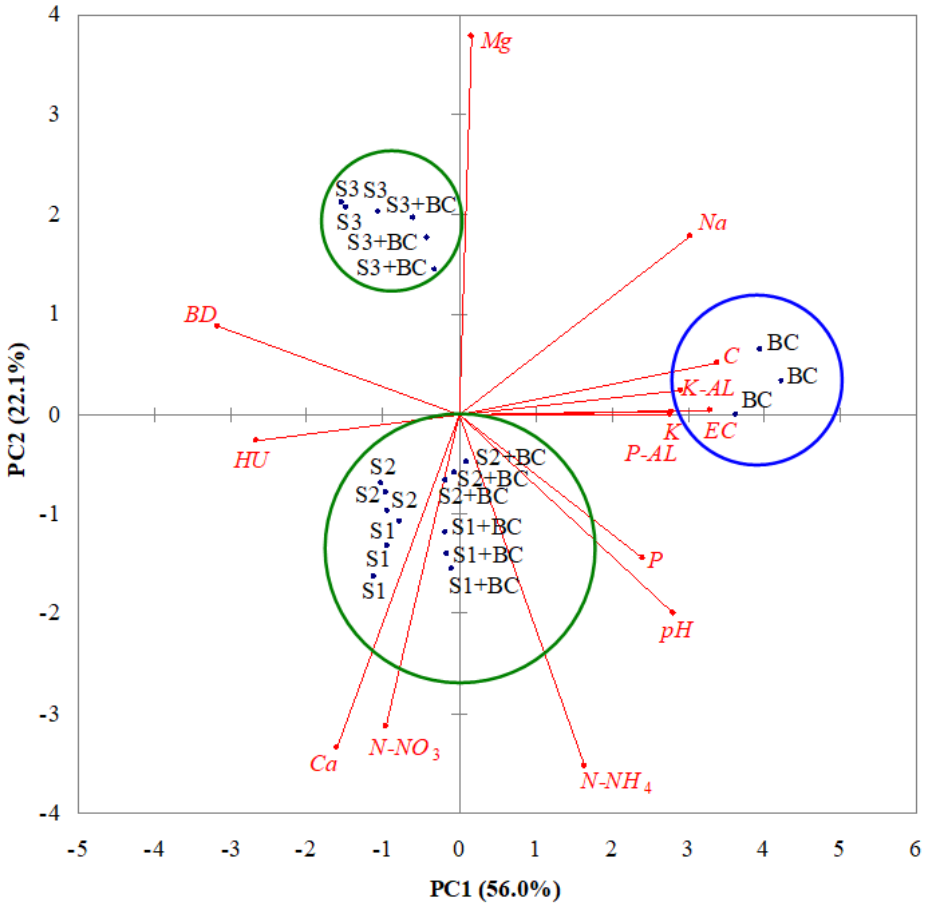


Figure 52. Projection of variables (*HU, BD, pH, EC, C, N-NO₃, N-NH₄, P, K, P-AL, K-AL, Ca, Mg,* and *Na*) and samples (S1, S2, S3, BC, S1 + BC, S2 + BC, and S3 + BC) on the PC1 and PC2 axes; (*HU*) humidity, (*BD*) bulk density, (*EC*) electrical conductivity, (*C*) total carbon content, (*N-NO₃*) soluble nitrate nitrogen concentration, (N-*NH₄*) soluble ammonium nitrogen concentration, (*P*) soluble phosphorus concentration, (*K*) soluble potassium concentration, (*P-AL*) mobile phosphorus concentration, (*K-AL*) mobile potassium concentration, (*Ca*) mobile calcium concentration, (*Mg*) mobile magnesium concentration, (*Na*) mobile sodium concentration, (BC) biochar, (S1) alluvial soil, (S2) chernozem, (S3) luvisol, (F) and (F/2) foliar fertilizer (0.2 mL/100 mL water and 0.1 mL/100 mL water) (Calcan et al., 2022b).

2.2.2.2.2. Effect of BC on plant growth characteristics

The levels of temperature inside and outside the greenhouse were 19.0±1.4 °C and 4.0±4.0 °C, respectively. Mean values±SD of tomato plant height (*H*), number of leaves (*NL*), collar diameter (*CD*), and root volume (*RV*) corresponding to 5 treatments (C, BC, F, BC+F, and BC+F/2) for each soil type, after 67 days from sowing, are presented in Figure 53.

BC had a beneficial effect on *H* of plants grown in soil 3 as well as a detrimental effect on *H* of plants grown in soils 1 and 2 (Figure 53a). Mean value of height (H_m) of plants grown in BC-amended soil 3 without fertilizer treatment (BC), *i.e.*, 21.3 cm, was about 50% higher than H_m of plants grown in soil 3 without and with fertilizer treatment (C and F) as well as about 30% higher than H_m of plants grown in BC-amended soil 3 with both fertilizer treatments (BC+F and BC+F/2). Plants grown in BC-amended soil 1 without and with fertilizer treatments (BC, BC+F, and BC+F/2) had similar mean values of height (H_m≈18 cm), about 40% and 30% lower than H_m of plants grown in soil 1 without and with fertilizer treatment (C and F). Plants grown in soil 2 without and with fertilizer treatment (C and F) had similar mean values of height (H_m≈18 cm), up to about 40% higher than those of plants grown in BC-amended soil 2 without and with fertilizer treatments (BC, BC+F, and BC+F/2).

BC had a beneficial effect on *NL* of plants grown in soil 3 and no favourable effect on *NL* of plants grown in soils 1 and 2 (Figure 53b). Mean value of number of leaves (NL_m) of plants grown in BC-amended soil 3 without fertilizer treatment (BC), *i.e.*, 7.5, was up to 25% higher than NL_m of plants grown in soil 3 without and with fertilizer treatment (C and F), as well as 9% higher than NL_m of plants grown in BC-amended soil 3 with both fertilizer treatments (BC+F and BC+F/2). Plants grown in BC-amended soils 1 and 2 without and with fertilizer treatments (BC, BC+F, and BC+F/2) had similar NL_m (7.0-7.3 and 5.4-5.8), 3-7% and 20-40% lower than NL_m of plants grown in soils 1 and 2 without and with fertilizer treatment (C and F).

BC had a favourable effect on *CD* of plants grown in soil 3 and no beneficial effect on *CD* of plants grown in soil 1 (Figure 53c). Mean value of collar diameter (CD_m) of plants grown in BC-amended soil 3 without fertilizer treatment (BC), *i.e.*, 3.1 mm, was about 20% higher than CD_m of plants grown in soil 3 without and with fertilizer treatment (C and F), as well as up to 12% higher than CD_m of plants grown in BC-amended soil 3 with both fertilizer treatments (BC+F and BC+F/2). Plants grown in BC-amended soil 1 without and with fertilizer treatments (BC, BC+F, and BC+F/2) had similar CD_m (3.0-3.1 mm), 5-14% lower than the CD_m of plants grown in soil 1 without and with fertilizer treatment (C and F). CD_m of plants grown in soil 2 with F and BC+F treatments were almost equal (2.8 mm and 2.9 mm, respectively) and 9-18% higher than CD_m of plants grown in soil 2 without and with other treatments (C, BC, BC+F/2).

The results depicted in Figure 53d indicate that BC had a favourable effect on the *RV* of plants grown in all soil types. Mean value of root volume (RV_m) of plants grown in soil 3 with BC+F/2 treatment, *i.e.*, 0.58 cm^3, was up to 2.8 times higher than RV_m of plants grown in soil 3 without treatment (C) and with fertilizer treatment (F) as well as up to 41% higher than RV_m of plants grown in soil 3 with other treatments (BC and BC+F). RV_m of plants grown in soil 1 with BC+F/2 treatment, *i.e.*, 0.51 cm^3, was 16-76% larger than RV_m of plants grown in soil 1 without and with other treatments (C, F, BC, and BC+F). RV_m of plants grown in BC-amended soil 2 with both fertilizer treatments (BC+F and BC+F/2) were almost equal (0.38 cm^3 and 0.37 cm^3, respectively) and were 1.4-2.1 times larger than those of plants grown in soil 2 without and with other treatments (C, F, and BC).

The results obtained revealed that H_m, NL_m, and CD_m of plants grown in soil 3 with BC treatment (BC) were up to 50% higher than those of plants grown in soil 3 without and with other treatments (C, F, BC+F, and BC+F/2). Figure 54 contains images of tomato plants grown for 66 days in untreated and treated strongly acidic soil 3. RV_m of plants grown in soil 3 with BC treatment (BC) was 32% lower than RV_m of plants grown in soil 3 with BC+F/2 treatment and up to 2.1 times higher than RV_m of plants grown in soil 3 without and with other treatments. Accordingly, very strongly alkaline BC (*pH* of 9.89±0.01) had a significant beneficial effect on *H*, *NL*, *CD*, and *RV* of plants grown in strongly acidic soil 3 (*pH* of 5.40±0.02).

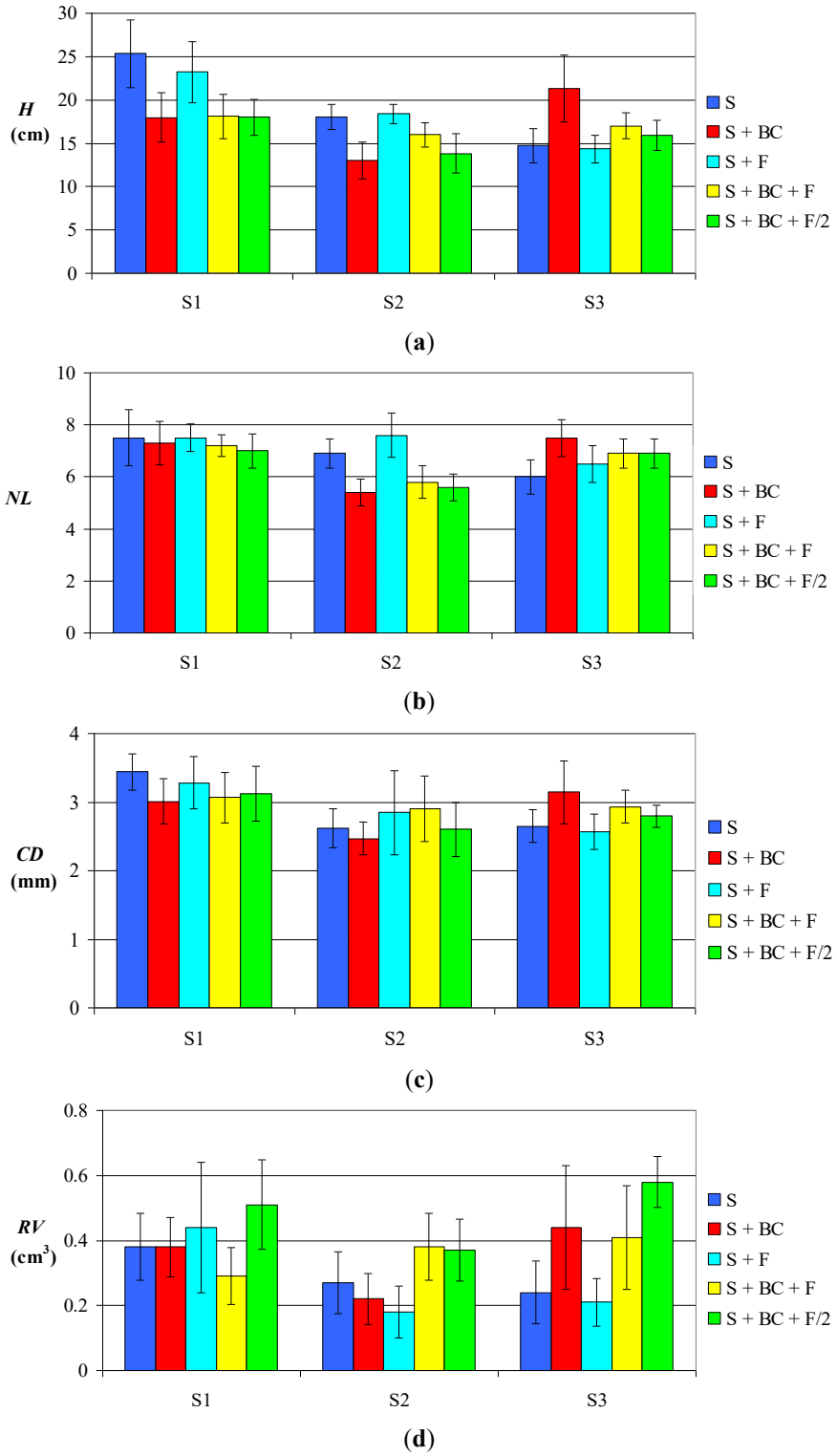


Figure 53. Mean values ± SD of tomato plant height (a), number of leaves (b), collar diameter (c), and root volume (d) at 66 days after sowing: (BC) biochar, (S1) alluvial soil, (S2) chernozem, (S3) luvisol, (F) and (F/2) foliar fertilizer (0.2 mL/100 mL water and 0.1 mL/100 mL water).

2.2.3. CONCLUSIONS

Strongly alkaline biochar (BC) ($pH = 9.89 \pm 0.01$), obtained by slow pyrolysis of vine prunings, had a significant beneficial effect on the growth characteristics of tomato plants sown in the strongly acidic soil S3 ($pH = 5.40 \pm 0.02$).

BC caused an increase in the electrical conductivity and *pH* of soil S3 from 0.094 ± 0.002 dS/m and 5.40 ± 0.02 to 0.158 ± 0.006 dS/m and 6.45 ± 0.11, resulting in a more favorable environment for plant growth. It also increased the concentrations of potassium (*K*) and phosphorus (*P*) in soluble and mobile forms (up to 8 times), as well as the concentrations of ammonium nitrogen ($N\text{-}NH_4$) in soluble form and sodium (*Na*) in mobile form (which were up to 26% higher).

Additionally, the application of BC reduced the bulk density of soil S3 from 1.314 ± 0.036 g/cm³ to 0.873 ± 0.038 g/cm³, which may have important beneficial effects on root development and, consequently, on plant growth by enhancing water and nutrient uptake.

BC had no favourable effect on *H*, *NL*, and *CD* of plants grown in moderately alkaline soil 1 and slightly acidic soil 2. Untreated soil 1 (C) was a more appropriate growing medium than soil 1 with fertilizer treatment (F) and moderately alkaline BC-amended soil 1 (*pH* of 8.33 ± 0.03) without and with fertilizer treatment (BC, BC+F, BC+F/2). Soil 2 with fertilizer treatment (F) was a more suitable option than untreated soil 2 (C) and neutral BC-amended soil 2 (*pH* of 7.10 ± 0.03) without and with fertilizer treatment.

The results obtained in this study suggest that application of very strongly alkaline BC as an organic amendment to strongly acidic soils is a promising strategy for enhancing soil quality, improving tomato plant growth, recovering nutrients from biomass residues, and mitigating climate change.

3. GENERAL CONCLUSIONS AND RESEARCH PERSPECTIVES

The PhD thesis (***VALORIZATION OF AGRO-INDUSTRIAL RESIDUES THROUGH PYROLYSIS***) comprises two main parts, i.e., **1. LITERATURE REVIEW**, which presents relevant aspects of the pyrolysis process, and **2. ORIGINAL CONTRIBUTIONS**, which include the results obtained in the author's own research on the production, characterization, and testing of biochar produced in a laboratory-scale installation (Chapter 2.1) and in a pilot laboratory-scale installation (Chapter 2.2).

Chapter 2.1. SLOW PYROLYSIS OF AGRO-INDUSTRIAL RESIDUES IN A LABORATORY INSTALLATION contains information related to the production of biochar in a laboratory installation, its characterization, and its testing as an adsorbent for volatile organic compounds (VOCs) from an air stream. Chapter 2.1 was structured into two parts: one focused on the production and characterization of biochar (Subchapter 2.1.1), and the other on the production, characterization, and testing of biochar modified (activated) by impregnating the feedstock with alkaline or acidic solutions (Subchapter 2.1.2).

In **Subchapter 2.1.1. Production and physicochemical characterization of biochar**, experimental and processed data are presented regarding the production of biochar from residual materials (vine prunings, grape marc, and chrysanthemum residues), as well as the characterization of both the plant residues and the biochar.

Slow pyrolysis of biomass residues was carried out in a pyrolysis column (3 cm inner diameter, 50 cm height) with a fixed bed of plant material, at 1 atm, in the presence of CO_2 as a carrier gas and oxidizing agent, for 1 hour.

An experimental study, based on a **2^3 factorial design**, was performed on the pyrolysis of shredded vine prunings (average diameter × average length: 3.5 mm × 20 mm and 7.0 mm × 20 mm). The process factors were: heat flux (q = 4244–5777 W/m²), CO_2 superficial velocity (w = 0.004–0.008 m/s), and volumetric mean particle diameter of the plant material (d = 0.007–0.011 m). The specific solid and liquid phase masses (m/m_0 and m_L/m_0) defined as the mass of pyrolytic product divided by the initial mass of plant residue, and the average fixed bed temperature (t_m) were selected as process responses. The results obtained highlighted the following aspects:

- The values of t_m and m_L/m_0 were higher, and those of m/m_0 lower, at the higher level of factor q (5777 W/m²).
- The values of m_L/m_0 were higher, and those of m/m_0 lower, at a higher level of factor d (0.011 m) and a lower level of factor w (0.004 m/s).
- Factor d had a negligible influence on t_m, and the effect of factor w on t_m was negligible for coarse particles (d = 0.011 m).
- The final response values of t_m (t_{mf} = 401.1–486.5 °C) were higher, while those of m/m_0 (m_f/m_0 = 0.286–0.328) were lower, at higher levels of factors q and d, as well as at the lower level of factor w.
- The final response values of mL/m₀ (m_{Lf}/m_0 = 0.260–0.350) were higher at higher levels of factors q and d.

The effects of the dimensionless factors, *i.e.*, $x_1 = \frac{q - 5010}{766}$, $x_2 = \frac{w - 0{,}006}{0{,}002}$ and $x_3 = \frac{d - 0{,}009}{0{,}002}$, and their interactions on the final response values, *i.e.*, $y_1 = (m_f/m_0)_{calc}$, $y_2 = (m_{Lf}/m_0)_{calc}$ și $y_3 = t_{mf,calc}$, were quantified using multiple regression equations. Statistical analysis revealed the following:

- x_2 had a significant positive effect and x_3 a significant negative effect on response y_1;
- x_3 had a significant positive effect, while x_1x_2, x_1x_3 and $x_1x_2x_3$ had negative effects on response y_2;

- x_2 had a significant negative effect, x_3 a significant positive effect, and x_1x_3 and x_2x_3 had significant positive effects on response y_3;
- Good agreement was observed between experimental and calculated data ($R^2 \geq 0{,}979$, $R^2_{adj} \geq 0{,}930$, $F \geq 20{,}08$ și $p \leq 0{,}016$).

The plant material samples (vine prunings, grape marc, and chrysanthemum residues) and biochar were characterized using specific analytical methods, *i.e.:*

- Concentrations of dry matter (*DM*), ash (*Ash*), volatile matter (*VM*), fixed carbon (*FC = DM − Ash − VM*), and water holding capacity (*WHC*) were determined by gravimetric methods.
- The concentrations of carbon (*C*), hydrogen (*H*), nitrogen (*N*), sulfur (*S*), and oxygen (*O = 100 – C – H – N – S*) were determined by elemental analysis;
- The concentrations of phosphorus (*P*), potassium (*K*), calcium (*Ca*), magnesium (*Mg*), aluminum (*Al*), boron (*B*), copper (*Cu*), iron (*Fe*), manganese (*Mn*), and zinc (*Zn*) were determined by inductively coupled plasma optical emission spectrometry (ICP–OES), while cobalt (*Co*) and molybdenum (*Mo*) concentrations were determined by inductively coupled plasma mass spectrometry (ICP–MS);
- Electrical conductivity (*EC*) and *pH* were measured using the SevenExcellence pH/EC meter;
- Bulk density (*BD*) was calculated as the ratio between the dry mass and volume of the sample;
- Morphology and functional groups were analyzed using SEM and FT-IR techniques.

The results obtained from the characterization of biochar derived from vine prunings (BC-V), grape marc (BC-T), and chrysanthemum residues (BC-C), processed using PCA, highlighted the following relevant aspects:

- BC-T samples showed higher values of *DM, FC, N, BD*, and *pH* variables, but lower *VM* and *O* values compared with BC-C samples;
- BC-V samples showed higher *C* values, but lower *EC, Ash*, and *H* values compared with BC-T samples;
- BC-T and BC-C samples had higher values *of K, Al, B, Co, Cu, Fe,* and *Mn*, but lower *Mo* and *Zn* values compared with BC-V samples;
- BC-V and BC-T samples had higher *Ca, P*, and *Mg* values compared with BC-C samples.

Due to the low values of *BD* (0.112 ± 0.001 g/cm³) and *EC* (0.55 ± 0.03 dS/m), as well as the relatively high levels of *pH* (10.35 ± 0.06), *WHC* (58.99 ± 14.51%), *P* (6.142 ± 0.093 mg/g), *Ca* (14.52 ± 0.12 mg/g), and *Mg* (2.632 ± 0.026 mg/g), biochar obtained from vine prunings could be used as a soil amendment for acidic soils. Moreover, its structure can be modified by impregnating the feedstock with acid or base solutions, resulting in biochar designed for specific applications, e.g., environmental remediation.

Subchapter 2.1.2. Production, characterization, and testing as adsorbent of biochar modified (activated) by impregnating the feedstock with alkaline or acidic solutions includes experimental and processed data related to the production of activated biochar via slow pyrolysis of vine prunings impregnated with KOH or H_3PO_4 solutions, as well as the characterization and testing of the activated char as an adsorbent for VOCs from an air stream.

Vine shoot residues with average dimensions of 3.5 mm × 20 mm (diameter × length) were impregnated with KOH solutions (10%, 20%, and 30%). The untreated and impregnated plant material was pyrolyzed in the presence of CO_2 (w = 0.4 cm/s), at q = 6.6 kW/m², 1 atm, for τ_f = 1 h. The biochars obtained at the end of the process (τ_f = 1 h) from untreated residues and residues impregnated with KOH solutions (10%, 20%, and 30%) were denoted BC, 10BC, 20BC, and 30BC, respectively.

Multivariate analysis (PCA) of the concentrations of carbon (*C*), hydrogen (*H*), nitrogen (*N*), oxygen (*O*), potassium (*K*), and phosphorus (*P*) of the BC, 10BC, 20BC, and 30BC samples revealed the following:

- 20BC and 30BC samples had higher *O* and *K* values, but lower *C, N*, and *P* values compared with BC;
- 10BC had higher *H* values compared with BC, 20BC, and 30BC;
- *C* and *N, C* and *P, N* and *P, O* and *K* were strongly positively correlated ($0{,}923 \leq r \leq 0{,}993$);
- *C* and *O, C* and *K, N* and *O, N* and *K, O* and *P, K* and *P* were strongly negatively correlated ($-1{,}000 \leq r \leq -0{,}911$).

Vine prunings residues with average dimensions of 3.5 mm × 20 mm were also impregnated with H_3PO_4 solutions (10%, 31%, 48%, and 52%). The impregnation ratio, $IR = m_{acid}/m_{rez}$, where m_{acid} and m_{rez} represent the masses of H_3PO_4 and plant residue, respectively, had values of 0.3 g/g, 1.1 g/g, 1.9 g/g, and 2.2 g/g. The untreated and impregnated plant material was pyrolyzed in the presence of CO_2 (w = 0.4 cm/s), at 1 atm, for 1 h.

According to a CCD experimental design with 2 factors, *i.e., IR* (0–2.2 g/g) and q (4.3–6.6 kW/m²), 12 slow pyrolysis experiments were carried out. The final values (τ_f = 1 h) of the specific solid phase masses (m_f/m_0 = 0.310–0.542 g/g) and liquid phase masses (m_{Lf}/m_0 = 0.230–0.334 g/g), as well as the final value of the mean bed temperature (t_{mf} = 345–422 °C), were selected as process responses. The solid phases obtained at the end of the process (τ_f = 1 h) from untreated and H_3PO_4-impregnated residues were denoted BC (biochar) and ABC (activated biochar), respectively.

BC and ABC samples obtained in the 12 pyrolysis experiments were tested as adsorbents of 1,2-dichloroethane (DCE) from an air stream. The final value (f) (at $\tau_{f,ads}$ = 90 min) of the adsorption capacity of BC/ABC for the VOC species (DCE), *i.e.,* $C_{if,ads}$ = 0.064–0.136 g/g, was selected as the adsorption process response.

The effects of the dimensionless factors $x_1 = \frac{q - 5{,}4}{0{,}8}$, $x_2 = \frac{IR - 1{,}1}{0{,}8}$, x_1^2, x_2^2 and the interaction x_1x_2 on $y_1 = (m_f/m_0)_{calc}$, $y_2 = (m_{Lf}/m_0)_{calc}$, $y_3 = t_{mf,calc}$ and $y_4 = C_{if,ads,calc}$ were quantified using second-order polynomial models. Statistical analysis of the results indicated the following:

- a significant positive effect of factor x_2 and significant negative effects of factors x_1, x_1^2 and x_2^2 on response y_1;
- a significant positive effect of factor x_1 and a significant negative effect of factor x_2 on response y_2;
- a significant positive effect of factor x_1 on response y_3;
- a significant negative effect of factor x_2^2 and significant positive effects of factors x_1, x_1^2 and x_2 on response y_4;
- good agreement between experimental and calculated data ($R^2 \geq 0{,}866$, $R^2_{adj} \geq 0{,}754$, $F \geq 7{,}735$, $p \leq 0{,}014$).

The optimal factor levels, for which the maximum calculated adsorption capacity value (y_4 = 0.137 g/g) was obtained, were x_1= 1.414 and x_2 = 0 (q = 6.6 kW/m² and IR = 1.1 g/g). At these optimal levels, maximum calculated response values of y_2 = 0.318 g/g and y_3 = 420 °C were obtained.

Chapter 2.2. SLOW PYROLYSIS OF AGRO-INDUSTRIAL RESIDUES IN A PILOT LAB-SCALE INSTALLATION presents data on the production of biochar in a pilot lab-scale installation, its characterization, and its testing as a soil amendment.

Slow pyrolysis of vine prunings with average dimensions of 0.7 cm × 6 cm (diameter × length) was performed in a pyrolysis furnace (inner diameter 15.5 cm, height 27 cm) with a

fixed bed of plant material, in the presence of CO_2 as carrier gas and oxidizing agent (w = 1.5 cm/s), at a temperature of 517 ± 16 °C, 1 atm, for 1 h.

The biochar obtained was ground to ≤ 2 mm particle size and then mixed with three types of clayey soils (pre-ground to ≤ 2 mm), namely:

- slightly alkaline alluvial soil S1 (pH = 7.99 ± 0.01);
- slightly acidic chernozem S2 (pH = 6.26 ± 0.02);
- strongly acidic luvisol S3 (pH = 5.40 ± 0.02).

The soil (S)/biochar (BC) mixing ratio was 4/1 v/v, corresponding to a BC application rate of 56 t/ha. The effects of applying strongly alkaline biochar (BC) (pH = 9.89 ± 0.01) on the physicochemical properties of soils and tomato plant growth characteristics were evaluated.

Soil samples (S1, S2, and S3), BC, and BC-amended soils (S1 + BC, S2 + BC, and S3 + BC) were characterized using specific analytical methods, *i.e.:*

- humidity (*HU*) was determined gravimetrically;
- electrical conductivity (*EC*) and *pH* were measured with a SevenExcellence pH/EC meter;
- bulk density (*BD*) was calculated as the ratio between the mass and volume of dried samples;
- total carbon concentration (*C*) was measured using an EA3100 elemental analyzer (Eurovector);
- soluble nitrate nitrogen (*N-NO₃*), soluble ammonium nitrogen (*N-NH₄*), and soluble phosphorus (*P*) concentrations were determined using a CECIL 2041 spectrophotometer (Buck Scientific);
- soluble potassium (*K*) concentration was measured using a Sherwood 410 flame photometer (Sherwood Scientific);
- available phosphorus and potassium concentrations (*P-AL* and *K-AL*) were determined using the Egner-Riehm-Domingo extraction followed by the spectrophotometric method (for *P*) and flame photometric method (for *K*);
- available calcium, magnesium, and sodium concentrations (*Ca, Mg,* and *Na*) were determined using an Optima 8300 ICP-OES inductively coupled plasma optical emission spectrometer (PerkinElmer).

The results of the characterization of soil samples (S1, S2, and S3), BC, and BC-amended soils (S1 + BC, S2 + BC, and S3 + BC), processed using PCA, highlighted the following relevant aspects:

- BC showed higher values for the variables *C* (76.01 ± 0.68%), *EC* (2.044 ± 0.070 dS/m), *pH* (9.89 ± 0.01), *K-AL* (8200 ± 0 mg/kg), *P-AL* (1615 ± 7 mg/kg), *K* (3131 ± 183 mg/kg), *P* (16.03 ± 0.28 mg/kg), and *Na* (87.94 ± 5.97 mg/kg), but lower values for *BD* (0.319 ± 0.018 g/cm³) and *HU* (3.51 ± 0.18%) compared to unamended and BC-amended soils;
- soil 3 (S3) and BC-amended soil 3 (S3 + BC) had higher *Mg* values (572.2–607.5 mg/kg) and lower values for *N-NO₃* (8.0–9.7 mg/kg), *N-NH₄* (2.8–4.1 mg/kg), and *Ca* (2182–2373 mg/kg) compared to the other unamended and BC-amended soils (*Mg* = 302.6–388.1 mg/kg, *N-NO₃* = 10.6–32.8 mg/kg, *N-NH₄* = 11.0–14.1 mg/kg, and *Ca* = 2415–3035 mg/kg).

A greenhouse experiment was conducted for 66 days to evaluate the effects of the amendment (BC) on tomato growth (variety "oxheart"). Five treatments were applied for each soil type (15 treatments × 10 replicates per treatment):

- control (S);
- BC (S + BC);
- foliar fertilizer (0.2 mL/100 mL water) (S + F);
- BC + foliar fertilizer (0.2 mL/100 mL water) (S + BC + F);

- BC + foliar fertilizer (0.1 mL/100 mL water) (S + BC + F/2).

Tomato seeds were planted in unamended soils (S) and BC-amended soils (S + BC), which were placed in seedling trays with 32 cells (a total of 150 cells). Plant height (*H*), number of leaves (*NL*), stem diameter (*CD*), and root volume (*RV*), measured 66 days after sowing, were selected as dependent variables.

One-way ANOVA highlighted the following aspects:

- Strongly alkaline BC (pH = 9.89 ± 0.01) had a significant positive effect on tomato growth characteristics in strongly acidic soil S3 (pH = 5.40 ± 0.02); the mean values of *H, NL*, and *CD* for plants grown under the S3 + BC treatment were up to 50% higher than those of plants grown in untreated soil S3 or with other treatments (S3 + F, S3 + BC + F, and S3 + BC + F/2); the mean *RV* value for plants grown under the S3 + BC treatment was up to 2.1 times higher than the mean *RV* values obtained for plants grown in untreated soil S3 and with the treatments S3 + F and S3 + BC + F;
- Strongly alkaline BC (pH = 9.89 ± 0.01) did not have a beneficial effect on *H, NL*, and *CD* for plants grown in slightly alkaline soil S1 (pH = 7.99 ± 0.01) and slightly acidic soil S2 (pH = 6.26 ± 0.02); combining BC with other organic amendments (e.g., compost, manure) or reducing the BC dose and/or pyrolysis temperature could be suitable options for improving plant growth characteristics in slightly alkaline/acid soils.

The results obtained in the studies conducted within the doctoral thesis suggest that the valorization of grapevine prunings through pyrolysis, which are produced in large quantities in Romania, is a promising strategy for reducing biomass residues, remediating the environment, improving soil quality, and enhancing plant growth.

The research carried out so far can be continued/deepened in future studies. The main objectives/directions of research I aim to pursue further refer to: the production of BC through slow pyrolysis of marine residues (e.g., macroalgal residues resulting from extraction processes, beach macroalgae) and its characterization; impregnation of BC derived from plant/marine residues with organic impregnation agents (e.g., compost tea, liquid digestate obtained through anaerobic fermentation of aquaculture sludge) and characterization of impregnated BC; testing unimpregnated/impregnated BC obtained as a soil amendment and/or adsorbent for environmental contaminants.

PAPER LIST

Published papers in ISI-indexed/journal-ranked journals used in the thesis:

1. Calcan, S.I., Pârvulescu, O.C., Ion, V.A., Răducanu, C.E., Bădulescu, L., Madjar, R., Dobre, T., Egri, D., Moț, A., Iliescu, L.M., Jerca, I.O. (2022) *Effects of biochar on soil properties and tomato growth*. Agronomy, 12(8), art. no. 1824, WOS:000846311700001 (Q1, **FI 2022= 3,7**).

2. Calcan, S.I., Pârvulescu, O.C., Ion, V.A., Răducanu, C.E., Bădulescu, L., Dobre, T., Egri, D., Moț, A., Popa, V., Crăciun, M.E. (2022) *Valorization of vine prunings by slow pyrolysis in a fixed-bed reactor*. Processes, 10(1), art. no. 37, WOS:000757674900001 (**FI 2022 = 3,5**).

3. Ion, V.A., Moț, A., Popa, V.I., **Calcan, S.**, Bădulescu, L., Jerca, I.O., Baniţă, C., Pârvulescu, O.C. (2021) *Physicochemical characterisation of vine waste used for producing biochar*. Sci. Papers Ser. B Hortic., LXV(2), 268–273, WOS:000756054100036.

4. Calcan, S.I., Pârvulescu, O.C., Ion, V.A., Răducanu, C.E., Dobre, T., Vasilievici, G., Burghelea, A. (2025) *Vine residue-derived engineered biochar for environmental benefits*. U.P.B. Sci. Bull. Series B, 87(3), ISSN 141-2331 (**FI 2024 = 0,3**).

Papers published in ISI-indexed/ranked journals from which information was used in the thesis:

5. Egri, D., Pârvulescu, O.C., Ion, V.A., Răducanu, C.E., Calcan, S.I., Bădulescu, L., Madjar, R., Orbeci, C., Dobre, T., Moț, A., Iliescu, L.M., Crăciun, M.E. (2022) Vine pruning-derived biochar for agronomic benefits. Agronomy, 12(11), art. no. 2730 (Q1, FI 2022 = 3,7).

6. Popovici, V., Bucur, L., **Calcan, S.I**., Cucolea, E.I., Costache, T., Rambu, D., Schroder, V., Gîrd, C.E., Gherghel, D., Vochita, G., D., Caraiane, A., Badea, V. (2022) *Elemental analysis and in vitro evaluation of antibacterial and antifungal activities of Usnea barbata (L.) Weber F.H. Wigg from Călimani Mountains, Romania.* Plants, 11(1), art. no. 32 (Q1, **FI 2022 = 5**).

7. Popovici, V., Bucur, L., Gîrd, C.E., **Calcan, S.I**., Cucolea, E.I., Costache, T., Rambu, D., Ungureanu-Iuga, M., Oroian, M., Mironeasa, S., Schroder, V., Ozon, E.A., Caraiane, A., Badea, V. (2022) *Advances in the characterization of Usnea barbata (L.) Weber F.H. Wigg from Călimani Mountains, Romania.* Applied Sciences, 12(9), art. no. 4234 (**FI 2022 = 2,7**).

8. Popovici, V., Bucur, L., Gîrd, C.E., Rambu, D., **Calcan, S.I**., Cucolea, E.I., Costache, T., Ungureanu-Iuga, M., Oroian, M., Mironeasa, S., Schroder, V., Ozon, E.A., Lupuliasa, D., Caraiane, A., Badea, V. (2022) *Antioxidant, cytotoxic, and rheological properties of canola oil extract of Usnea barbata (L.) Weber F.H. Wigg from Călimani Mountains, Romania.* Plants, 11(7), art. no. 854 (Q1, **FI 2022 = 5**).

9. Popovici, V., Bucur, L., Vochita, G., Gherghel, D., Mihai, C.T., Rambu, D., **Calcan, S.I**., Costache, T., Cucolea, E.I., Matei, E., Badea, F.C., Caraiane, A., Badea, V. (2021) *In vitro anticancer activity and oxidative stress biomarkers status determined by Usnea barbata (L.) F.H. Wigg dry extracts.* Antioxidants, 10(7), art, no. 1141 (Q1, **FI 2021 = 7,7**).

IMPACT FACTOR

1–4: **7,5**

5–9: **24,1**

TOTAL: 31,6

Oral presentations (O)/posters (P) at international conferences/symposia:

1. Calcan, S.I., Răducanu, C.E., Pârvulescu, O.C., Ion, V.A., Răducanu, C.E., Egri, D., Dobre, T. *Valorisation of vine branches by slow pyrolysis*. 16th International Conference of Constructive Design and Technological Optimization in Machine Building Field (OPROTEH), 25-27 May 2021, Bacau, Romania (P).

2. Ion, V.A., Mot, A., Popa, V.I., **Calcan, S.I.**, Bădulescu, L., Jerca, O., Banita, C., Pârvulescu, O.C. (2021) *Physicochemical characterisation of vine waste used for producing biochar*. International Conference "Agriculture for Life, Life for Agriculture", 4-6 June 2021, Bucharest,

Romania (P).

3. Ion, V.A., Pârvulescu, O.C., Moț, A., Popa, V.I., **Calcan, S.I.,** Răducanu, C.E., Bădulescu, L., Grigoraș, C. (2021) *Valorization of greenhouse biomass waste using pyrolysis*. International Conference "Intelligent Valorisation of Agro-Industrial Wastes (INTELWASTES)", 7-8 October 2021, Chisinau, Republic of Moldova (P).

4. Calcan, S.I., Pârvulescu, O.C., Ion, V.A., Răducanu, C.E., Bădulescu, L., Roxana Madjar, R., Dobre, T., Egri, D., Moț, A., Iliescu, L.M., Jerca, I.O. *Production of biochar and its use as an amendment for acidic soils*. 17th International Conference of Constructive Design and Technological Optimization in Machine Building Field (OPROTEH), 25-27 May 2022, Bacau, Romania (P).

5. Ion, V.A., Moț, A., Popa, V.I., **Calcan, S.I.,** Bădulescu, L., Marin, S.M., Răducanu, C.E., Pârvulescu, O.C. *Pyrolysis of grape marc waste for producing biochar*. International Conference "Agriculture for Life, Life for Agriculture", 2-4 June 2022, Bucharest, Romania (P).

6. Pârvulescu, O.C., Ion, V.A., Răducanu, C.E., Egri, D., **Calcan, S.I.,** Orbeci, C., Dobre, T., Madjar, R., Bădulescu, L., Moț, A., Iliescu, L.M. *Effects of biochar on soil properties and pepper growth*. 22nd Romanian International Conference on Chemistry and Chemical Engineering (RICCCE 22), 7-9 September 2022, Sinaia, Romania (P).

7. Răducanu, C.E., Pârvulescu, O.C., Ion, V.A., Dobre, T., Burghelea, A., Negrea, A., **Calcan, S.I.,** Egri, D. *Engineered biochar for environmental benefits*. 22nd Romanian International Conference on Chemistry and Chemical Engineering (RICCCE 22), 7-9 September 2022, Sinaia, Romania (P).

8. Egri, D., Pârvulescu, O.C., Ion, V.A., Bădulescu, L., **Calcan, S.I**., Dobre, T., Răducanu, C.E., Mocanu, A., Løes, A.K., Cabell, J., Salifoglou, A., Maroulis, M., Matsia, S., Letelier-Gordo, C.O., Carboni, F.M. *Biochar amendment applied to improve crop growth and yield*. International Chemical Engineering and Material Symposium (SICHEM), 17-18 November 2022, Bucharest, Romania (P).

9. Popovici, V., Bucur, L., Gîrd, C.E., Rambu, D., **Calcan, S.I.,** Cucolea, E.I., Costache, T., Ungureanu-Iuga, M., Oroian, M., Mironeasa, S., Schroder, V., Ozon, E.A., Lupuliasa, D., Caraiane, A., Badea, V. *Valorization of autochthonous lichen Usnea barbata (L.) to obtain an enriched canola oil extract*. Conference Sustainable Food: Trends and Opportunities, online workshop, October 2023 (O).

10. Popovici, V., Bucur, L., **Calcan, S.I**., Gîrd, C.E., Ozon, E.A., Musuc, A.M., Morosan, E., Surdu, I. *Elemental analysis and heavy metals content of Usnea barbata (L.) Weber F.H. Wigg from Călimani Mountains*. 10th International Conference ESPERA, 23-24 November 2023 (P).

11. Calcan S.I., Pârvulescu O.C., Ion V.A., Dobre T. *Effects of biochar derived from vine residues on plant growth*. 20th International Conference of Constructive Design and Technological Optimization in Machine Building Field (OPROTEH), 21-23 May 2025, Bacau, Romania (O).

SELECTIVE REFERENCES

1. Abi Bianasari, A., Khaled, M. S., Hoang, T. D., Reza, M. S., Bakar, M. S. A., & Azad, A. K. (2024). Influence of combined catalysts on the catalytic pyrolysis process of biomass: A systematic literature review. *Energy Conversion and Management*, *309*, 118437.
2. Amalina, F., Abd Razak, A. S., Krishnan, S., Sulaiman, H., Zularisam, A. W., & Nasrullah, M. (2022). Biochar production techniques utilizing biomass waste-derived materials and environmental applications–A review. *Journal of Hazardous Materials Advances*, *7*, 100134.
3. Ansari, K. B., Kamal, B., Beg, S., Khan, M. A. W., Khan, M. S., Al Mesfer, M. K., & Danish, M. (2021). Recent developments in investigating reaction chemistry and transport effects in biomass fast pyrolysis: A review. *Renewable and Sustainable Energy Reviews*, *150*, 111454.
4. Bahng, M. K., Mukarakate, C., Robichaud, D. J., & Nimlos, M. R. (2009). Current technologies for analysis of biomass thermochemical processing: A review. *Analytica Chimica Acta*, *651*(2), 117-138.
5. Balat, M., Balat, M., Kırtay, E., & Balat, H. (2009). Main routes for the thermo-conversion of biomass into fuels and chemicals. Part 1: Pyrolysis systems. *Energy Conversion and Management*, *50*(12), 3147-3157.
6. Bedia García-Matamoros, J., Peñas-Garzón, M., Gómez Avilés, A., Rodríguez Jiménez, J. J., & Belver Coldeira, C. (2018). A review on the synthesis and characterization of biomass-derived carbons for adsorption of emerging contaminants from water. C *(Journal of Carbon Research), 4*(4), 63.
7. Biswas, B., Pandey, N., Bisht, Y., Singh, R., Kumar, J., & Bhaskar, T. (2017). Pyrolysis of agricultural biomass residues: Comparative study of corn cob, wheat straw, rice straw and rice husk. *Bioresource Technology*, *237*, 57-63.
8. Bridgwater, A.V. (2012). Review of fast pyrolysis of biomass and product upgrading. *Biomass and Bioenergy*, *38*, 68-94.
9. Bru, K., Blin, J., Julbe, A., Volle, G. (2007) Pyrolysis of metal impregnated biomass: An innovative catalytic way to produce gas fuel. *J. Anal. Appl. Pyrolysis, 78,* 291–300.
10. Calcan, S. I., Pârvulescu, O. C., Ion, V. A., Răducanu, C. E., Bădulescu, L., Dobre, T., Egri, D., Moț, A., Popa, V., & Crăciun, M. E. (2022a). Valorization of vine prunings by slow pyrolysis in a fixed-bed reactor. *Processes*, *10*(1), 37.
11. Calcan, S. I., Pârvulescu, O. C., Ion, V. A., Răducanu, C. E., Bădulescu, L., Madjar, R., Dobre, T., Egri, D., Moț, A., & Iliescu, L. M. (2022b). Effects of biochar on soil properties and tomato growth. *Agronomy*, *12*, 1824.
12. Calcan, S. I., Pârvulescu, O. C., Ion, V. A., Răducanu, C. E., Dobre, T., Vasilievici, G., & Burghelea, A. (2025). Vine residue-derived engineered biochar for environmental benefits. *U.P.B. Sci. Bull.* Series B, *87*(3), 135-148.
13. Çağlar, A., Demirbaş, A. (2002a) Hydrogen rich gas mixture from olive husk via pyrolysis. *Energ. Convers. Manage*., 43, 109–117.
14. Çağlar, A., Demirbaş, A. (2002b) Conversion of cotton cocoon shell to hydrogen rich gaseous products by pyrolysis. *Energ. Convers. Manage*., 43, 489–497.
15. Chen, W., Meng, J., Han, X., Lan, Y., & Zhang, W. (2019a). Past, present, and future of biochar. *Biochar*, *1*, 75-87.
16. Chen, X., Che, Q., Li, S., Liu, Z., Yang, H., Chen, Y., ... & Chen, H. (2019b). Recent developments in lignocellulosic biomass catalytic fast pyrolysis: Strategies for the optimization of bio-oil quality and yield. *Fuel Processing Technology*, *196*, 106180.

17. Collard, F. X., & Blin, J. (2014). A review on pyrolysis of biomass constituents: Mechanisms and composition of the products obtained from the conversion of cellulose, hemicelluloses and lignin. *Renewable and Sustainable Energy Reviews*, *38*, 594-608.
18. Cusenza M.A., Longo S., Cellura M., Guarino F., Messineo A., Mistretta M., Volpe M. (2021). Environmental assessment of a waste-to-energy practice: The pyrolysis of agro-industrial biomass residues. *Sustainable Production and Consumption*, *28*, 866-876.
19. Demirbaş, A. (2002a) Gaseous products from biomass by pyrolysis and gasification: Effects of catalyst on hydrogen yield. *Energ. Convers. Manage., 43,* 897–909.
20. Demirbaş, A. (2002b) Partly chemical analysis of liquid fraction of flash pyrolysis products from biomass in the presence of sodium carbonate. *Energ. Convers. Manage., 43*, 1801–1809.
21. Demirbaş, A. (2006) Effect of temperature on pyrolysis products from four nut shells, *J. Anal. Appl. Pyrolysis, 76*, 285–289.
22. Di Blasi, C. (1998) Comparison of semi-global mechanisms for primary pyrolysis of lignocellulosic fuels. *J. Anal. Appl. Pyrolysis, 47*(1), 43–64.
23. Di Blasi, C. (2008). Modeling chemical and physical processes of wood and biomass pyrolysis. *Progress in Energy and Combustion Science*, *34*(1), 47-90.
24. Dobre, T., Parvulescu, O. C., Ramos, I. R., Ceatră, L., Stroescu, M., Stoica, A., & Mirea, R. (2012). Global reaction kinetics and enthalpy in slow pyrolysis of vegetal materials. *Revista de Chimie*, *63*(1), 54-59.
25. Dobre, T., Pârvulescu, O. C., Iavorschi, G., Stoica, A., & Stroescu, M. (2010). Catalytic effects at pyrolysis of wheat grains impregnated with nickel salts. *International Journal of Chemical Reactor Engineering*, *8*(1), 1968–1992.
26. Dobre, T., Pârvulescu, O. C., Iavorschi, G., Stroescu, M., & Stoica, A. (2014). Volatile organic compounds removal from gas streams by adsorption onto activated carbon. *Industrial & Engineering Chemistry Research*, *53*(9), 3622-3628.
27. Dobre, T., Pârvulescu, O. C., Jacquemet, A., & Ion, V. A. (2016). Adsorption and thermal desorption of volatile organic compounds in a fixed bed–Experimental and modeling. *Chemical Engineering Communications*, *203*(12), 1554-1561.
28. Egri, D., Pârvulescu, O. C., Ion, V. A., Răducanu, C. E., Calcan, S. I., Bădulescu, L., Madjar, R., Orbeci, C., Dobre, T., Moț, A. et al. (2022) Vine pruning-derived biochar for agronomic benefits. *Agronomy*, *12*(11), 2730.
29. El Bari, H., Fanezoune, C. K., Dorneanu, B., Arellano-Garcia, H., Majozi, T., Elhenawy, Y., ... & Ashour, F. H. (2024). Catalytic fast pyrolysis of lignocellulosic biomass: Recent advances and comprehensive overview. *Journal of Analytical and Applied Pyrolysis*, *178*, 106390.
30. El Hanandeh, A., Mahdi, Z., & Imtiaz, M. S. (2021). Modelling of the adsorption of Pb, Cu and Ni ions from single and multi-component aqueous solutions by date seed derived biochar: Comparison of six machine learning approaches. *Environmental Research*, *192*, 110338.
31. Garcia, L., French, R., Czernik, S., Chornet, E. (2000) Catalytic steam reforming of bio-oils for the production of hydrogen: Effects of catalyst composition. *Applied Catalysis A: General, 201*, 225–239.
32. Ghosh, P., Sengupta, S., Singh, L., & Sahay, A. (2020). Life cycle assessment of waste-to-bioenergy processes: A review. *Bioreactors*, 105-122.
33. Gwenzi, W., Chaukura, N., Wenga, T., & Mtisi, M. (2021). Biochars as media for air pollution control systems: Contaminant removal, applications and future research directions. *Science of the Total Environment*, *753*, 142249.

34. Hameed, S., Sharma, A., Pareek, V., Wu, H., & Yu, Y. (2019). A review on biomass pyrolysis models: Kinetic, network and mechanistic models. *Biomass and Bioenergy*, *123*, 104-122.
35. Kan, T., Strezov, V., & Evans, T. J. (2016). Lignocellulosic biomass pyrolysis: A review of product properties and effects of pyrolysis parameters. *Renewable and Sustainable Energy Reviews*, *57*, 1126-1140.
36. Kechagiopoulos, P.N., Voutetakis, S.S., Lemonidou, A.A., Vasalos, I.A. (2006) Hydrogen production via steam reforming of the aqueous phase of bio-oil in a fixed bed reactor. *Energy&Fuels, 20*(5), 2155–2163.
37. Kechagiopoulos, P.N., Voutetakis, S.S., Lemonidou, A.A., Vasalos, I.A. (2007) Sustainable hydrogen production via reforming of ethylene glycol using a novel spouted bed reactor. *Catalysis Today, 127*(1–4), 246–255.
38. Khan, A., Szulejko, J. E., Samaddar, P., Kim, K. H., Liu, B., Maitlo, H. A., ... & Ok, Y. S. (2019). The potential of biochar as sorptive media for removal of hazardous benzene in air. *Chemical Engineering Journal*, *361*, 1576-1585.
39. Khan, M. B., Cui, X., Jilani, G., Tang, L., Lu, M., Cao, X., ... & He, Z. (2020). New insight into the impact of biochar during vermi-stabilization of divergent biowastes: Literature synthesis and research pursuits. *Chemosphere*, *238*, 124679.
40. Kimura, L. M., Santos, L. C., Vieira, P. F., Parreira, P. M., & Henrique, H. M. (2010). Biomass pyrolysis: Use of some agricultural wastes for alternative fuel production. In *Materials Science Forum* (vol. 660, pp. 259-264). Trans Tech Publications Ltd.
41. Lee X. J., Lee L. Y., Gan S., Thangalazhy-Gopakumar S., & Ng, H. K. (2017). Biochar potential evaluation of palm oil wastes through slow pyrolysis: Thermochemical characterization and pyrolytic kinetic studies. *Bioresource Technology*, *236*, 155-163.
42. Lee, J., Sarmah, A. K., & Kwon, E. E. (2019). Production and formation of biochar. In *Biochar from Biomass and Waste* (pp. 3-18). Elsevier.
43. Lehmann, J., & Joseph, S. (2015). Biochar for environmental management: an introduction. In *Biochar for Environmental Management* (pp. 1-13). Routledge.
44. Mlonka-Mędrala, A., Evangelopoulos, P., Sieradzka, M., Zajemska, M., & Magdziarz, A. (2021). Pyrolysis of agricultural waste biomass towards production of gas fuel and high-quality char: Experimental and numerical investigations. *Fuel*, *296*, 120611
45. Oliveira, F. R., Patel, A. K., Jaisi, D. P., Adhikari, S., Lu, H., & Khanal, S. K. (2017). Environmental application of biochar: Current status and perspectives. *Bioresource Technology*, *246*, 110-122.
46. Parihar, M.F., Kamil, M., Goyal, H.B., Gupta, A.K., Bhatnagar, A.K. (2007) An experimental study on pyrolysis of biomass. *Trans IChemE, 85*(B5), 458–465.
47. Pârvulescu, O. C., Dobre, T., Ceatră, L., Iavorschi, G., & Mirea, R. (2011) Characteristics of corn grains pyrolysis in a fixed bed reactor. *Revista de Chimie*, *62*(1), 89-94.
48. Pârvulescu, O. C., Gavrilă, A. I., Dobre, T., & Ceatră, L. (2016). Effects of process factors on slow pyrolysis of sorghum waste. *Revista de Chimie*, *67*(11), 2254-2257.
49. Qian, K., Kumar, A., Zhang, H., Bellmer, D., & Huhnke, R. (2015). Recent advances in utilization of biochar. *Renewable and Sustainable Energy Reviews*, *42*, 1055-1064.
50. Rangabhashiyam, S., & Balasubramanian, P. (2019). The potential of lignocellulosic biomass precursors for biochar production: Performance, mechanism and wastewater application—A review. *Industrial Crops and Products*, *128*, 405-423.
51. Rehman, I., Riaz, M., Ali, S., Arif, M. S., Ali, S., Alyemeni, M. N., & Alsahli, A. A. (2021). Evaluating the effects of biochar with farmyard manure under optimal mineral fertilizing on tomato growth, soil organic C and biochemical quality in a low fertility soil. *Sustainability*, *13*(5), 2652.

52. Richardson, Y., Blin, J., Volle, G., Motuzas, J., Julbe, A. (2010) In situ generation of Ni metal nanoparticles as catalyst for H_2-rich syngas production from biomass gasification. *Applied Catalysis A: General, 382*, 220–230.
53. Tang Q., Chen Y., Yang H., Liu M., Xiao H., Wang S., Chen H., & Naqvi S. R. (2021). Machine learning prediction of pyrolytic gas yield and compositions with feature reduction methods: Effects of pyrolytic conditions and biomass characteristics. *Bioresource Technology*, *339*, 125581.
54. Tian, B., Wang, J., Qiao, Y., Huang, H., Xu, L., & Tian, Y. (2023). Understanding the pyrolysis synergy of biomass and coal blends based on volatile release, kinetics and char structure. *Biomass and Bioenergy*, *168*, 106687.
55. Tian, B., Xu, L., Jing, M., Liu, N., & Tian, Y. (2021). A comprehensive evaluation on pyrolysis behavior, kinetics, and primary volatile formation pathways of rice husk for application to catalytic valorization. *Fuel Processing Technology*, *214*, 106715.
56. Tomczyk, A., Sokołowska, Z., & Boguta, P. (2020). Biochar physicochemical properties: pyrolysis temperature and feedstock kind effects. *Reviews in Environmental Science and Bio/Technology*, *19*(1), 191-215.
57. Tripathi, N., Hills, C. D., Singh, R. S., & Atkinson, C. J. (2019). Biomass waste utilisation in low-carbon products: harnessing a major potential resource. *NPJ climate and atmospheric science*, *2*(1), 35.
58. Usino, D. O., Ylitervo, P., Moreno, A., Sipponen, M. H., & Richards, T. (2021). Primary interactions of biomass components during fast pyrolysis. *Journal of Analytical and Applied Pyrolysis*, *159*, 105297.
59. Verma, M., Godbout, S., Brar, S. K., Solomatnikova, O., Lemay, S. P., & Larouche, J. P. (2012). Biofuels production from biomass by thermochemical conversion technologies. *International Journal of Chemical Engineering*, *2012*(1), 542426.
60. Wang, B., Gao, B., & Fang, J. (2017). Recent advances in engineered biochar productions and applications. *Critical Reviews in Environmental Science and Technology*, *47*(22), 2158-2207.
61. Wang, Z., Wang, Q., Yang, X., Xia, S., Zheng, A., Zeng, K., ... & Werle, S. (2021). Comparative assessment of pretreatment options for biomass pyrolysis: Linking biomass compositions to resulting pyrolysis behaviors, kinetics, and product yields. *Energy & Fuels*, *35*(4), 3186-3196.
62. Wu, C., Yan, Y., Li, T., & Qi, W. (2007) Preparation of hydrogen through catalytic steam reforming of bio-oil. *Chinese Journal of Process Engineering*, *7*(6), 1114-1119.
63. Wu, W., Kawamoto, K., & Kuramochi, H. (2006). Hydrogen-rich synthesis gas production from waste wood via gasification and reforming technology for fuel cell application. *Journal of Material Cycles and Waste Management*, *8*, 70-77.
64. Wu, C., Yan, Y., Li, T., Qi, W. (2007) Preparation of hydrogen through catalytic steam reforming of bio-oil. *Chinese Journal of Process Engineering, 7*, 1114–1119.
65. Wu, W., Yang, M., Feng, Q., McGrouther, K., Wang, H., Lu, H., & Chen, Y. (2012). Chemical characterization of rice straw-derived biochar for soil amendment. *Biomass and Bioenergy*, *47*, 268-276.
66. Xu, C. Y., Li, Q. R., Geng, Z. C., Hu, F. N., & Zhao, S. W. (2020). Surface properties and suspension stability of low-temperature pyrolyzed biochar nanoparticles: Effects of solution chemistry and feedstock sources. *Chemosphere*, *259*, 127510.
67. Yaashikaa, P. R., Kumar, P. S., Varjani, S., & Saravanan, A. J. B. R. (2020). A critical review on the biochar production techniques, characterization, stability and applications for circular bioeconomy. *Biotechnology Reports*, *28*, e00570.
68. Yang, F., Wang, W., Wu, Z., Peng, J., Xu, H., Ge, M., ... & Peñuelas, J. (2024). Fertilizer reduction and biochar amendment promote soil mineral-associated organic carbon,

bacterial activity, and enzyme activity in a jasmine garden in southeast China. *Science of the Total Environment*, *954*, 176300.
69. Yang, H., Yan, R., Chen, H., Lee, D. H., & Zheng, C. (2007). Characteristics of hemicellulose, cellulose and lignin pyrolysis. *Fuel*, *86*(12-13), 1781-1788.
70. Yang, H., Yan, R., Chen, H., Zheng, C., Lee, D. H., & Liang, D. T. (2006). In-depth investigation of biomass pyrolysis based on three major components: Hemicellulose, cellulose and lignin. *Energy & Fuels*, *20*(1), 388-393.
71. Yang, Y., Sun, C., Lin, B., & Huang, Q. (2020). Surface modified and activated waste bone char for rapid and efficient VOCs adsorption. *Chemosphere*, *256*, 127054.
72. Yi, W., Liu, L., Wang, D., Zhang, X., & Yu, G. (2025). Potential of biochar derived from sewage sludge and calcium sulfate as an amendment for acidic soils: Milk Chinese cabbage cultivation. *Journal of Environmental Chemical Engineering*, *13*(2), 115641.
73. Yi, Z., Li, C., Lin, H., Zhang, S., Huang, Y., Li, B., ... & Hu, X. (2023). Pyrolysis of sawdust impregnated with bio-oil of the same origin: influence of organics in bio-oil on property of biochar. *Biomass and Bioenergy*, *178*, 106961.
74. Yin, R., Liu, R., Mei, Y., Fei, W., & Sun, X. (2013). Characterization of bio-oil and bio-char obtained from sweet sorghum bagasse fast pyrolysis with fractional condensers. *Fuel*, *112*, 96-104.
75. Yogalakshmi, K. N., Sivashanmugam, P., Kavitha, S., Kannah, Y., Varjani, S., AdishKumar, S., & Kumar, G. (2022). Lignocellulosic biomass-based pyrolysis: A comprehensive review. *Chemosphere*, *286*, 131824.
76. Yu, F., Ruan, R., Steele, P. (2008) Consecutive reaction model for the pyrolysis of corn cob. Trans. ASABE, 51, 1023–1028.
77. Yu, X., Wang, X., Sun, M., Liu, H., Liu, D., & Dai, J. (2024). Cadmium immobilization in soil using phosphate modified biochar derived from wheat straw. *Science of The Total Environment*, *926*, 171614.
78. Yuan, P., Wang, J., Pan, Y., Shen, B., & Wu, C. (2019). Review of biochar for the management of contaminated soil: Preparation, application and prospect. *Science of the Total Environment*, *659*, 473-490.
79. Yung, M.M., Jablonski, W.S., Magrini-Bair, K.A. (2009) Review of catalytic conditioning of biomass-derived syngas. Energy&Fuels, 23, 1874–1887.
80. Zanzi, R. (2001) *Pyrolysis of biomass*. Dissertation, Royal Institute of Technology, Stockholm.
81. Zhang, C., Liu, N., Zhang, T., Su, S., Li, R., Feng, J., & Wu, Y. (2025). Influence of biomass type and pyrolysis temperature on biochar characteristics for enhanced soil amendment. *Journal of Analytical and Applied Pyrolysis*, *192*, 107257.
82. Zhang, K., Zhang, K., Li, Y., Kang, Q., Wang, Y., Wang, J., ... & Mao, J. (2023). Easily pyrolyzable biomass components significantly affect the physicochemical properties and water-holding capacity of the pyrolyzed biochar. *Agriculture*, *13*(11), 2053.
83. Zhao, Z., Wang, B., Theng, B. K., Lee, X., Zhang, X., Chen, M., & Xu, P. (2022). Removal performance, mechanisms, and influencing factors of biochar for air pollutants: A critical review. *Biochar*, *4*(1), 30.